Targeting BRCA2 deficiency with GSK3 inhibitors

Gijs Zonderland

Lincoln College

A thesis submitted to the University of Oxford for the degree of

Master of Science by Research

Trinity Term 2017

CRUK and MRC Oxford Institute for Radiation Oncology

Department of Oncology

University of Oxford

Content

Acknowledgments

I would like to thank my supervisors Dr. Madalena Tarsounas and Dr. Anderson Ryan for their support during my studies. My academic and scientific expertise has grown significantly thanks to this experience. Additionally, I am thankful for having been able to attend the 2017 Genome Stability Network meeting in Cambridge.

A special thanks goes to Lincoln College for supporting me throughout my time in Oxford. Particularly, I would like to thank Prof. Bass Hassan for his support and advise. Also, I would like to thank Director of Graduate Studies Prof. Ester Hammond for her guidance.

Many thanks to all the lab members I have worked with for the past year. All of you made my life in the lab enjoyable and productive. It was the friendship we created in the lab that kept me going. I will always remember the fun times we have had together.

I want to give a huge thanks to my family and friends! Thanks to my family for their immense support and belief in me. My experiences and studies would not have been possible without them.

Lastly, my biggest thank you goes to the most important person in my life, Jutta. Your blind trust, endless support, strong belief and love in me gave me so much strength. There are no words to describe how grateful I am for having you in my life, you mean the absolute world to me!

Abstract

BRCA1 and BRCA2 tumour suppressors are essential for homologous recombination-mediated double-strand break repair and replication fork protection. Therefore, BRCA1 and BRCA2 are essential for cell viability. Deactivating mutations in one of these genes lead to genome instability and are associated with breast and ovarian cancer. We thus performed a chemical library screen and identified glycogen synthase kinase 3 (GSK3) inhibitors as a potent tool to kill BRCA2-deficient cells.

One of the best-characterised cellular functions of serine/threonine kinase GSK3 is its role in the WNT pathway. Here, it acts as a regulator of β-catenin, with the inactivation of GSK3 leading to the stabilisation of β-catenin.

In this study, we show that inhibition of GSK3 reduces the viability of human BRCA2-deficient cells. In addition, GSK3 inhibition leads to replication stress, DNA damage and genome instability in the context of BRCA2 deficiency. GSK3 inhibition sensitivity can be reversed by depleting β-catenin. Furthermore, GSK3 inhibition-induced replication stress and checkpoint activation is reduced when β-catenin is depleted.

BRCA1-deficient cells that have lost 53BP1 are able to overcome PARP inhibitor olaparib sensitivity by reactivating homologous recombination. Interestingly, we find that olaparib-resistant *Brca1*$^{-/-}$, 53BP1-deficient cells are sensitive to GSK3 inhibition, whilst *Brca1*$^{+/+}$ cells remain unaffected.

In summary, these results demonstrate that GSK3 inhibitors may be used to target HR deficiency, including cells that have acquired resistance against currently used therapies.

Declaration

Hereby, I declare that the work presented in this study is wholly my own.

Nomenclature

Human genes are indicated in upper case italic lettering (e.g. *BRCA2*).

Mouse genes are indicated in italic with the first letter in upper case and the remaining letters in lower case (e.g. *Brca2*).

Human and mouse proteins are indicated in upper case lettering (e.g. BRCA2).

Abbreviations

˚C	degree(s) Celsius
53BP1	p53-binding protein 1
APC	adenomatous polyposis coli
ATM	ataxia telangiectasia mutated protein
ATR	ataxia telangiectasia and RAD3-related protein
BLM	Bloom's syndrome protein
BRCA	breast cancer susceptibility protein, e.g. BRCA1
BSA	bovine serum albumin
CHD4	chromodomain helicase DNA-binding protein 4
CHK1	checkpoint kinase 1
CK1	casein kinase 1
CldU	5-chloro-2'deoxyuridine
cm	centimetre(s)
CtIP	CTBP-interacting protein
CTR	control
D-loop	displacement loop
DAPI	4',6-diamidino-2-phenylindole
DMEM	Dulbecco's modified Eagle medium
DNA	deoxyribonucleic acid
DNA2	DNA replication helicase 2
DOX	doxycycline
DSB	double-strand break
dsDNA	double-stranded DNA
DTT	dithiothreitol
DVL	Dishevelled
ECL	enhanced chemiluminescence
EDTA	ethylene diamine tetraacetic acid
EdU	5-ethynyl-2'-deoxyuridine

EME1	essential meiotic structure-specific endonuclease 1
EXO1	exonuclease 1
F12	Ham's F-12 nutrient mixture
FBS	foetal bovine serum
g	acceleration due to gravity (on Earth 9.80665 m/s^2)
GAPDH	glyceraldehyde 3-phosphate dehydrogenase
GEN1	GEN1, Holliday junction 5' flap endonuclease
GSK3	glycogen synthase kinase 3
h	hour(s)
HELB	DNA helicase B
HR	homologous recombination
IB	immunoblotting
IC_{50}	half maximal inhibitory concentration
IdU	5-iodo-2'-deoxyuridine
IF	immunofluorescence
LRP5/6	Low-density lipoprotein receptor-related protein 5/6
LY	LY2090314
M	molar
min	minute(s)
mL	millilitre(s)
mM	millimolar
MOPS	3-morpholinopropane-1-sulfonic acid
MRE11	meiotic recombination 11
MRN	complex formed by MRE11, RAD50 and NBS1
MUS81	MUS81, structure-specific endonuclease
ng	nanogram(s)
NHEJ	non-homologous end joining
nm	nanometre(s)
nM	nanomolar
ns	not significant

NSB1	nibrin
p	phospho
PAGE	polyacrylamide gel electrophoresis
PALB2	partner and localizer of BRCA2
PARP	poly (ADP-ribose) polymerase
PBS	phosphate buffered saline
pH	potential of hydrogen
PTIP	Pax transactivation domain-interacting protein
RAD	radiation resistance protein, e.g. RAD51
REV7	MAD2L2, mitotic arrest deficient-like 2
RMI1	RecQ-mediated genome instability protein 1
RNA	ribonucleic acid
RNAi	RNA interference
RPA	replication protein A
RT	room temperature
S	serine
SD	standard deviation
SDS	sodium dodecyl sulphate
shRNA	small hairpin RNA
siRNA	small interfering RNA
SMC1	structural maintenance of chromosomes protein 1
ssDNA	single-stranded DNA
T	threonine
TCF/LEF	T-cell factor/lymphoid enhancer factor
TOPIIIα	topoisomerase III α
Tris	tris (hydroxymethyl) aminomethane
V	volt
X-ray	X-radiation
Y	tyrosine
β-cat	β-catenin

β-TrCP	FBXW1A, F-box/WD repeat-containing protein 1A
µg	microgram(s)
µL	microlitre(s)
µM	micromolar
µm	micrometre(s)

List of figures

List of tables

1 Introduction

Cancer is the disease that leads to the most deaths worldwide. In 2015, it cost 8.8 million individuals their life (WHO, 2017). Cancer is characterised by the uncontrolled growth of cells. A small modification in the DNA can cause the cell to start growing rapidly and become aggressive by invading multiple tissues.

This transformation can rise from DNA damage, which cells are exposed to throughout their life cycle (Lindahl et al., 2000). Besides by-products of cellular processes such as the immune response (Kawanishi et al., 2006) or oxidative respiration (Valko et al., 2006), exogenous sources like ultraviolet light can cause DNA damage (Jackson et al., 2009). DNA lesions occur in various ways and appear in different forms, among which double-strand breaks (DSBs) are the most detrimental. Accurate repair is necessary to preserve genome stability. Homologous recombination (HR) is an error-free mechanism for the repair of DSBs that most commonly uses the sister chromatid as a template to restore the original DNA sequence. Genes involved in HR are commonly mutated in tumours leading to genome instability, a hallmark of cancer (Negrini et al., 2010).

1.1 HR is required for genome stability

The key mechanism for accurate DSB repair is HR, which requires an intact, homologous DNA sequence as a template (Johnson et al., 2000; Johnson et al., 1999; Valerie et al., 2003). HR is not only vital for DSB repair but also for DNA replication, during which it is needed to protect, repair and restart stalled replication forks in a precise manner (Lomonosov et al., 2003; Nagaraju et al., 2007). Replication forks can stall as a consequence of DNA damage, proteins bound to DNA and secondary DNA structures. To protect stalled replication forks,

HR prevents nucleolytic degradation of nascent DNA mediated by MRE11 nuclease (Schlacher et al., 2011; Schlacher et al., 2012). In more severe cases, stalled replication forks collapse leading to DSB formation. HR is then required for the repair of the DSB followed by the reactivation of DNA synthesis (Arnaudeau et al., 2001; Segurado et al., 2002).

Two major proteins in HR are breast cancer susceptibility protein 1 (BRCA1) and breast cancer susceptibility protein 2 (BRCA2). Due to their role in HR, BRCA1 and BRCA2 are essential for cell viability (Hakem et al., 1996; Suzuki et al., 1997). Mutations in *BRCA1* and *BRCA2* have been implicated in breast and ovarian cancer (King et al., 2003; Welcsh et al., 2001). In addition, patients who have mutations in *BRCA1* or *BRCA2* display extreme levels of genome instability (Lord et al., 2016). This is presumably caused by inaccurate repair of DSBs.

1.1.1 Double-strand break repair by HR

The roles of BRCA1 and BRCA2 in DSB repair by HR have been studied extensively. The first step in DSB repair is the recognition of the break. Hereof, the MRE11-RAD50-NSB1 (MRN) complex binds to the DSB in approximately 13 seconds (Haince et al., 2008) and activates ataxia telangiectasia mutated protein (ATM) (Moreno-Herrero et al., 2005; Shiloh, 2003; Stracker et al., 2004). This triggers the DNA damage response, which acts as a safeguard to allow repair of the break before the cell cycle progresses (Lowndes et al., 2000).

There are two main pathways for the repair of DSBs, HR and non-homologous end joining (NHEJ). NHEJ, which is active throughout the cell cycle, is an error-prone repair mechanism. On the contrary, HR is error-free and only

active during S and G2 phase (Ahnesorg et al., 2006; Grawunder et al., 1997; Gu et al., 2007). During G1 phase, NHEJ is promoted by p53 binding protein 1 (53BP1) that inhibits resection (Bothmer et al., 2010; Bunting et al., 2010). HR is activated during S and G2 phase by BRCA1. The MRN complex, in concert with CtIP, initiates resection on both sides of the DSB (Huertas et al., 2008). Extensive resection is then mediated by BLM helicase and the nucleases DNA2 and EXO1 (Nimonkar et al., 2011; Nimonkar et al., 2008; Sartori et al., 2007). This generates single-stranded DNA (ssDNA) that is protected from degradation by replication protein A (RPA) (Chen et al., 2013). To initiate strand invasion into intact homologous double-stranded DNA (dsDNA), RPA is displaced by radiation resistance protein 51 (RAD51), which is loaded by BRCA2 (Moynahan et al., 2001) together with BRCA1 and PALB2 (Sy et al., 2009a; Sy et al., 2009b; Zhang et al., 2009). RAD51 forms nucleoprotein filaments and mediates strand invasion, leading to the formation of a displacement loop (D-loop) (Baumann et al., 1996; Sung, 1994; Sung et al., 1995). This causes the formation of Holiday junctions which need to be dissolved by BLM-TOPIIIα-RMI1 or resolved by GEN1 or MUS81-EME1, leading to crossover or non-crossover products (Boddy et al., 2001). The complete process of repairing a DSB by HR takes roughly 20 minutes (Mine-Hattab et al., 2012). An overview of the key activities during HR-mediated DSB repair is illustrated in Figure 1.1.

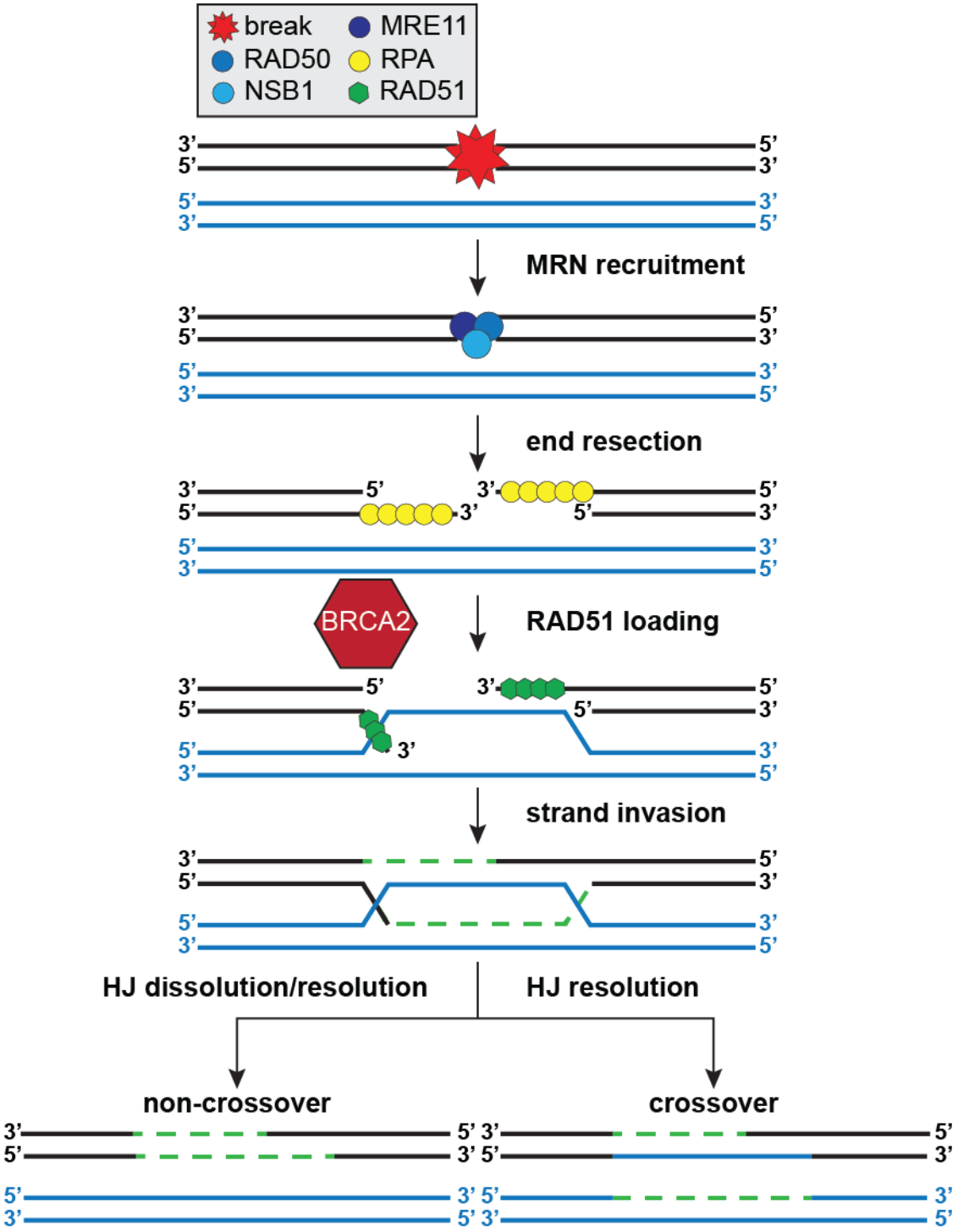

Figure 1.1. DSB repair by HR.
Once a DSB occurs, MRN binds to the break within 13 seconds and initiates resection. RPA coats the exposed ssDNA to protect it from degradation. BRCA2 loads RAD51 onto the ssDNA, thereby displacing RPA. RAD51 forms nucleofilaments and triggers strand invasion into the homologous dsDNA, leading to the formation of Holiday junctions (HJ). HJ are dissolved by BLM-TOPIIIα-RMI1 or resolved by GEN1 or MUS81-EME1, resulting in crossover or non-crossover products. The process from recognition of the break to the repair takes approximately 20 min.

1.1.2 Role of HR during DNA replication

BRCA1 and BRCA2 are essential proteins in the accurate repair of DSBs. Besides their role in HR, they are required during DNA replication (Lomonosov et al., 2003; Nagaraju et al., 2007). Problems that arise during DNA synthesis lead to a replication stress response (Zeman et al., 2014).

Replication stress is defined by the slowing down or stalling of the replication fork, resulting in long stretches of ssDNA (Zeman et al., 2014). These ssDNA stretches are usually formed when the replicative helicase continues to unwind the dsDNA even though the polymerase has stalled (Pacek et al., 2004). The replication stress response is activated when the ssDNA adjacent to the stalled replication fork persists (Byun et al., 2005). One of the central kinases in the replication stress response, which is recruited to these structures, is ataxia telangiectasia and Rad3 related (ATR). Recruitment of ATR to stalled forks leads to the phosphorylation and activation of checkpoint kinase 1 (CHK1) to inhibit cell cycle progression (Liu et al., 2000; Melo et al., 2002; Zhao et al., 2001; Zou et al., 2003b). In addition, ATR restrains late origin firing (Tercero et al., 2001). To prevent degradation of the ssDNA exposed at the replication fork by MRE11 nuclease, BRCA1 and BRCA2 are recruited to the replication fork to protect the nascent DNA (Figure 1.2) (Schlacher et al., 2011; Schlacher et al., 2012). After the source of stress has been removed, replication forks can be restarted (Petermann et al., 2010). However, the cell may fail to restart the replication fork because of persistence of the source. It is believed that these fail-to-restart replication forks collapse (Cobb et al., 2003; De Piccoli et al., 2012; Lopes et al., 2001; Ragland et al., 2013; Tercero et al., 2001). A collapsed replication fork can be transformed into a DSB. One way that a stalled replication fork is processed

into a DSB is through cleavage by endonucleolytic activity of MUS81 (Hanada et al., 2006). DSBs that arise from replication fork collapsing are primarily repaired by HR (Arnaudeau et al., 2001). In addition, HR activities are required to restart DNA synthesis (Figure 1.2) (Arnaudeau et al., 2001; Segurado et al., 2002).

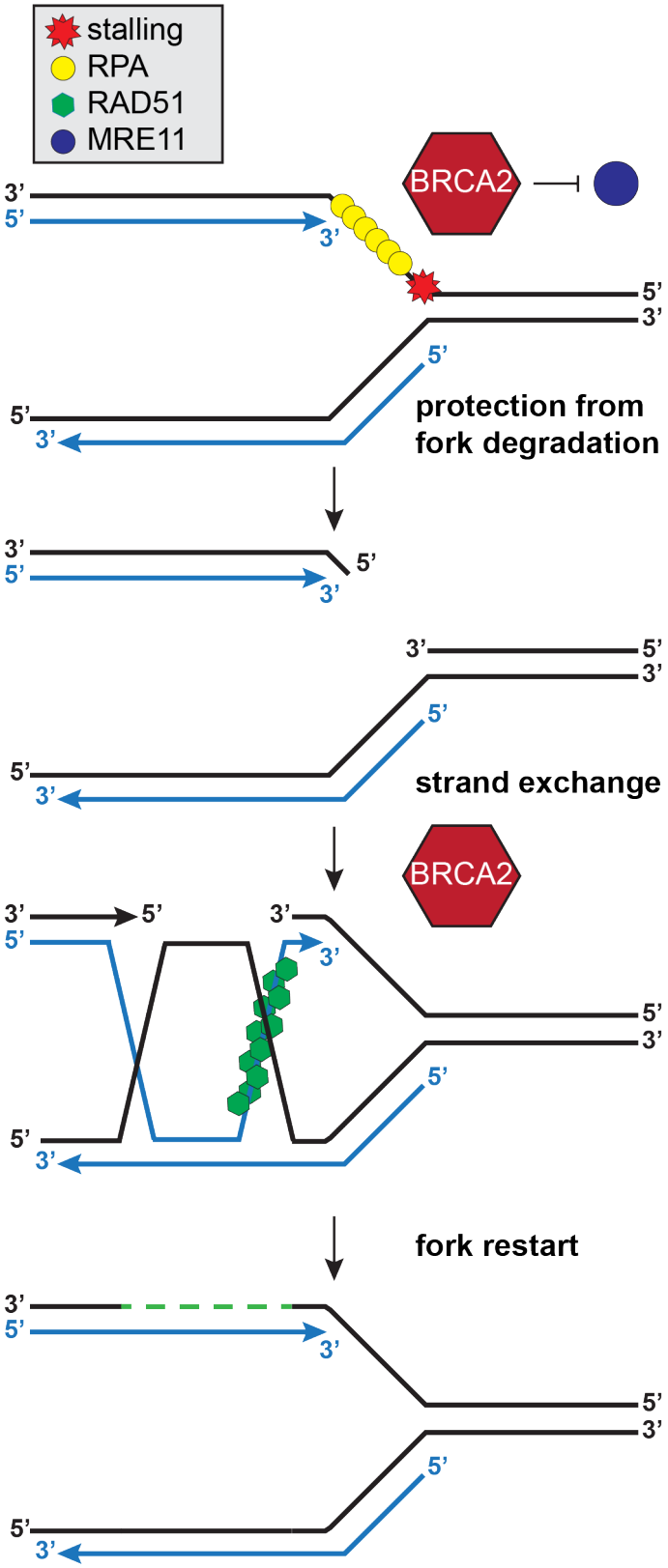

Figure 1.2. Fork protection and restart by HR.
When a replication fork stalls, RPA binds to the exposed ssDNA. BRCA2 prevents MRE11-mediated DNA degradation. Endonucleases cleave DNA at the fork, resulting in a HR-like reaction to repair the break.

1.1.3 Therapeutic targeting of HR-deficient tumours

Gene-inactivating mutations in either *BRCA1* or *BRCA2* are associated with high risk of breast and ovarian cancer (King et al., 2003; Welcsh et al., 2001). One explanation for the increased risk of developing cancer may be that the error-prone DSB repair mechanism NHEJ takes over when HR is inactive (Lord et al., 2016; Prakash et al., 2015). DSB repair by NHEJ often leads to insertions or deletions, which can lead to chromosome rearrangements (Lord et al., 2012; Simsek et al., 2010; Zhang et al., 2011). Therefore, BRCA-associated tumours exhibit high levels of genome instability (Lord et al., 2016). Currently, patients with HR-inactive tumours are usually treated with radiation and/or chemotherapy. These treatments rely on the incompetent repair of the induced DNA damage. Cells proficient in HR are capable of repairing the damage in an accurate way. This enables selectively targeting of HR-deficient tumour cells.

More recently, a promising approach has been exploited to treat different types of cancer, called synthetic lethality. Similarly to the aforementioned treatments that rely on inadequate DSB repair of HR-defective cells, the concept of synthetic lethality is based on defects in multiple genes that result in cell death. In brief, individual inactivation of two genes is tolerated but deletion of both genes simultaneously is not compatible with cell viability (Dobzhansky, 1946). Based on synthetic lethality, the inhibition of poly (ADP-ribose) polymerase (PARP) by olaparib was identified to specifically kill HR-deficient cells (Bryant et al., 2005; Farmer et al., 2005). PARP is involved in single-strand break repair (Fisher et al., 2007). Olaparib primarily targets PARP1-3 causing the trapping of PARP1-3 on the DNA. The persistence of PARP on the DNA can lead to fork stalling and collapse, causing DSB formation (Helleday, 2011). Cells defective in BRCA1 or

BRCA2 are unable to repair the collapsed fork. Healthy cells remain unaffected because they are capable of accurate repair by HR. This promising approach of targeting HR-deficient tumours by the inhibition of PARP provided encouraging results in clinical trials (Audeh et al., 2010; Fong et al., 2009; Tutt et al., 2010).

A major setback for the therapeutic approaches to treat BRCA-associated tumours has been the development of resistance. The high levels of genome instability in HR-defective cancers gives the cells an opportunity for rearrangements in *BRCA1* and *BRCA2* genes that can re-establish their functionality (Barber et al., 2013; Edwards et al., 2008; Sakai et al., 2008). This means that the cells regain HR function. Furthermore, other mechanisms have been identified that restore HR activity in BRCA1-deficient cells. These mechanisms rely on the restoration of resection through loss of 53BP1, its downstream target REV7 or helicase HELB (Boersma et al., 2015; Bouwman et al., 2010; Bunting et al., 2010; Cao et al., 2009; Tkac et al., 2016; Xu et al., 2015). RAD51 is then loaded onto the ssDNA overhangs by BRCA2 and HR is restored. More recently, another model of chemoresistance has been suggested, in which replication forks are stabilised in the absence of BRCA2 by silencing of PTIP, CHD4 or PARP, thereby preventing MRE11-mediated resection (Ding et al., 2016; Ray Chaudhuri et al., 2016). However, these cells are not able to reactivate HR. The findings of Ray Chaudhuri et al. (2016) suggest that fork stability in the absence of BRCA2 correlates with drug resistance.

Promising therapies have been identified that are able to selectively target resistant BRCA1-dysfunctional tumour cells (Yazinski et al., 2017; Zimmer et al., 2016). Yazinski et al. (2017) report that PARP-resistant BRCA1-deficient cells are sensitive to a combination treatment of ATR inhibition and PARP inhibitor

olaparib. Mechanistically, BRCA1-deficient cells resistant for PARP inhibition are able to load RAD51 after olaparib treatment (Yazinski et al., 2017; Zimmer et al., 2016). However, additional treatment with an ATR inhibitor prevents loading of RAD51 by disturbing the BRCA1, PALB2 and BRCA2 interaction (Buisson et al., 2017; Yazinski et al., 2017). Zimmer et al. (2016) found that treatment with pyridostatin, a G-quadruplex stabiliser, kills BRCA1-deficient cells resistant for PARP inhibition. In addition, pyridostatin treatment was suggested to prevent resection, which blocks RAD51 loading in BRCA1-, 53BP1-deficient cells (Zimmer et al., 2016).

Overall, current approaches and therapies to target BRCA-deficient tumours lack selectivity and are vulnerable to the development of resistance. To identify novel approaches to target these difficult-to-treat cancer cells, we performed a chemical library screen (Tacconi, 2015), in which we identified inhibitors of glycogen synthase kinase 3 (GSK3).

1.2 Role of GSK3 in the WNT pathway

GSK3 is a serine/threonine kinase that was first identified in 1980 (Embi et al., 1980), but only ten years later it became clear that GSK3 is involved in a great number of cellular processes such as stem cell renewal, apoptosis and cell proliferation (Hanger et al., 1992; Pei et al., 1997). Because of GSK3's multi-functionality, it is also involved in the onset and development of human diseases like cancer and bipolar mood disorder as well as life-long disorders such as diabetes, neurodegenerative diseases and muscle hypertrophy (Martinez, 2008; Patel et al., 2008; Takahashi-Yanaga, 2013). Remarkably, GSK3 is barely mutated in cells, suggesting that GSK3 may be a promising target to treat these

devastating diseases. Thus, various inhibitors of GSK3 have been synthesised, some of which have been tested in clinical trials (Cohen et al., 2004; Eldar-Finkelman et al., 2011; Frame et al., 2001; Meijer et al., 2004).

GSK3 exists of two genes, GSK3α and GSK3β. They are located on different chromosomes but are 85% homologous (Woodgett, 1990). The distinct function between the two genes is not very well studied. Nevertheless, a study in mice revealed that GSK3α knockout is viable, even though the mice displayed increase levels of insulin and glucose. In addition, GSK3α knockout mice had a reduced fat mass. In contrast, deletion of GSK3β in mice led to liver degradation after 16 days and was lethal (Hoeflich et al., 2000). Thus, this study suggests that GSK3α and GSK3β have separate functions.

Despite GSK3's role in other pathways, its function in the WNT pathway has been studied the most (Figure 1.3). Here, both GSK3α and GSK3β are required (Doble et al., 2007). In resting, non-proliferating cells, the WNT receptor Frizzled is unbound (Figure 1.3A). This leads to the activation of GSK3 by autophosphorylation of tyrosine (Y) 279 on GSK3α and Y216 on GSK3β (Cole et al., 2004). Active GSK3 forms a destruction complex together with CK1, APC, Axin and β-TrCP. Here, Axin scaffolds the destruction complex and CK1 phosphorylates β-catenin on serine (S) 45. Active GSK3 recognises phosphorylated β-catenin and further phosphorylates β-catenin on S33, S37 and threonine (T) 41 (Amit et al., 2002; Dominguez et al., 1995; He et al., 1995; Liu et al., 2002; Pierce et al., 1995). β-TrCP ubiquitinates phosphorylated β-catenin and targets it for proteasomal degradation (Hart et al., 1999; Kitagawa et al., 1999; Latres et al., 1999; Liu et al., 1999; Winston et al., 1999). On the other hand, when a WNT ligand binds to the Frizzled receptor, the WNT pathway is

activated (Figure 1.3B). The binding of the ligand to the receptor causes a dimer formation with the LRP5/6 receptor, leading to the inactivation of APC and Axin (Zeng et al., 2008). DVL prevents activation of GSK3 by phosphorylation of S21 and S9 on GSK3α and GSK3β, respectively (Cross et al., 1995; Cross et al., 1994; Stambolic et al., 1994; Sutherland et al., 1993). This causes the stabilisation of β-catenin, which is then transferred to the nucleus where it acts as an activator of transcription factors TCF/LEF (Novak et al., 1999). One of the proteins that is stimulated upon TCF/LEF-mediated transcription is the oncogene MYC (He et al., 1998).

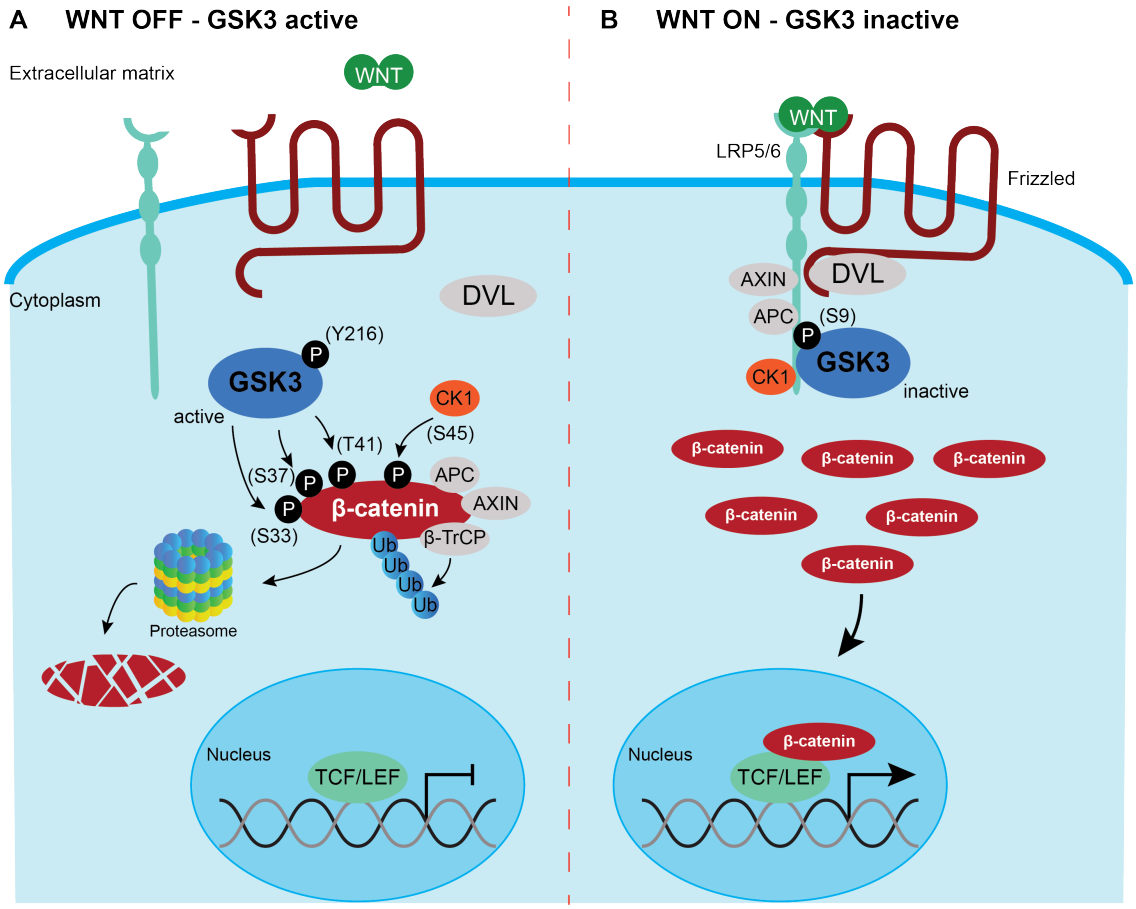

Figure 1.3. Overview of the WNT pathway.
(**A**) In the absence of WNT stimulation, GSK3 is activated by autophosphorylation. This leads to the formation of a destruction complex, containing GSK3, CK1, APC, Axin and β-TrCP. Here, Axin scaffolds the destruction complex and interacts with all components. APC is an essential protein in the complex, however, its exact role remains unclear. CK1 phosphorylates β-catenin on S45, which is recognised by GSK3. In turn, GSK3 phosphorylates β-catenin on S33, S37 and T41 leading to the ubiquitination of β-catenin mediated by β-TrCP. Finally, β-catenin is degraded by the proteasome. (**B**) When a WNT ligand binds to the Frizzled receptor, a dimer is formed with the LRP5/6 receptor. This leads to the activation of DVL, which inhibits the destruction complex, causing β-catenin stabilisation. β-catenin is then transferred into the nucleus where it acts as an activator of transcription factors TCF/LEF. Ub, ubiquitin; p, phosphorylated.

1.3 Aim of this study

A chemical library revealed GSK3 inhibitors as a potent tool to kill BRCA2-deficient cells (Tacconi, 2015). The aim of this study was to understand the mechanism by which the inhibition of GSK3 leads to the killing of BRCA2-deficient cells. First, the outcome of the library screen was validated in different cell lines lacking BRCA2. Secondly, we sought to investigate a potential synthetic lethal interaction between GSK3 and BRCA2. Thirdly, we monitored replication stress accumulation, replication dynamics and DNA damage induction upon GSK3 inhibition. Fourthly, we assessed the role of β-catenin in GSK3 inhibitor-treated cells. Lastly, we tested the potential of GSK3 inhibition in cells resistant to PARP inhibitor olaparib.

2 Materials and methods

2.1 Cell culture

Human colorectal adenocarcinoma DLD1 cells (parental and *BRCA2*-mutated; Horizon Discovery; Hucl et al. (2008)) and non-small lung carcinoma H1299 cells (America Type Culture Collection) were grown in Dulbecco's Modified Eagle's Medium (DMEM; Sigma-Aldrich #D5796). Media for DLD1 cells were supplemented with 10% fetal bovine serum (FBS; Invitrogen #10270-106) and 1% penicillin-streptomycin (Sigma-Aldrich #P4333). Media for H1299 cells were supplemented with 10% tetracycline-free FBS (Thermo Fisher Scientific #SH3007003) and 1% penicillin-streptomycin. Cells were cultured at 37˚C in 5% CO_2. H1299 cells expressing doxycycline (DOX)-inducible small hairpin RNA (shRNA) against BRCA2 were previously established in Prof. Madalena Tarsounas' lab (Zimmer et al., 2016) using the 'all-in-one' system, described by Wiederschain et al. (2009). Using lentiviral infection, BRCA2 shRNA (GGG AAA CAC TCA GAT TAA A) cloned into pLKO^{TetOn} vector were introduced into H1299 cells. Efficient BRCA2 knockdown was confirmed after eight days in the presence of 2 µg/mL DOX (Sigma-Aldrich #D9891). The mechanism of DOX-inducible shRNA-mediated depletion is shown in Figure 2.1. H1299 cells were grown in the presence or absence of DOX for three days before the start of an experiment.

Brca1$^{+/+}$ (KP3.33; *wild type*), *Brca1*$^{-/-}$ (KB1PM5; olaparib-sensitive) and *Brca1*$^{-/-}$, 53BP1-deficient (KB1PM5; olaparib-resistant) mouse mammary tumour-derived cell lines were cultured at 37˚C, 5% CO_2 and 3% O_2. All three cell lines were grown in DMEM/F-12 (Life Technologies #31331-028) supplemented with 10% FBS, 1% penicillin-streptomycin, 5 µg/mL insulin (Sigma-Aldrich #I0516-5ML), 5 ng/mL epidermal growth factor (Life Technologies #53003018) and 5

ng/mL cholera toxin (Gentaur #LST10). Cholera toxin was added to the cells as it has been shown to promote cell growth of epithelial cells by stimulating cyclic adenosine monophosphate levels (Okada et al., 1982; Stampfer, 1982).

Cells were detached using Trypsin-EDTA (Sigma-Aldrich #T3924) for 5 minutes (min) at 37˚C in 5% CO_2, after washing cells with phosphate-buffered saline (PBS; Fisher Scientific #BR0014). Cells were counted using a haemocytometer.

BRCA2-deficient DLD1 cells and their parental -proficient counterpart were used as a cell model for stable BRCA2 deficiency. In contrast, H1299 cells were used as an inducible model of BRCA2 deficiency mediated by DOX-inducible shRNA against BRCA2. These two models enabled us to assess the effect of GSK3 inhibitors in cells that have adapted to BRCA2 loss and in cells that suffer from prompt depletion of BRCA2. Importantly, DLD1 cells harbour a mutation in *APC*, resulting in higher endogenous levels of β-catenin (Tang et al., 2008), whilst H1299 cells are WNT pathway *wild type*. This allowed us to study GSK3 inhibitor sensitivity in cells that are mutated in the WNT pathway and in cells with a *wild type* WNT pathway. Additionally, KP3.33 (*Brca1*$^{+/+}$) and KB1PM5 (*Brca1*$^{-/-}$ and *Brca1*$^{-/-}$, 53BP1-deficient) mouse mammary tumour-derived cells were used as a model to study the effect of GSK3 inhibition on olaparib-resistant cells.

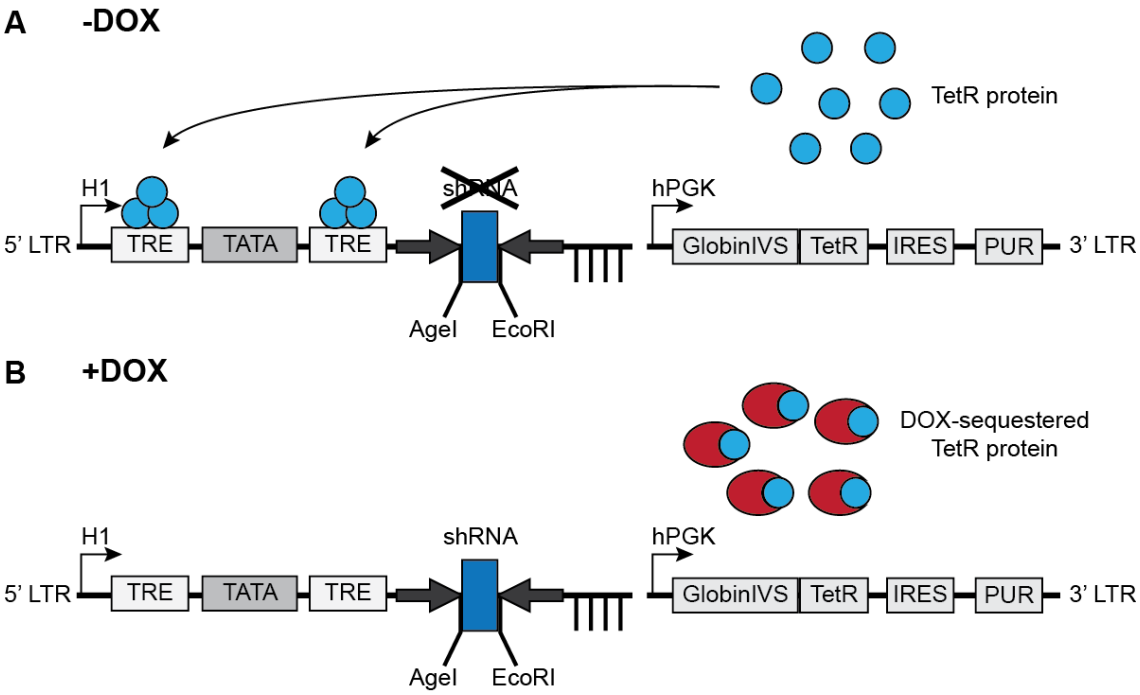

Figure 2.1. Mechanism of DOX-inducible shRNA-mediated protein depletion. (**A**) In the absence of DOX (-DOX), expression of shRNA is suppressed by constitutively expressed TetR protein. TetR binds to the TREs within the H1 promotor, thereby preventing shRNA expression. (**B**) In the presence of DOX (+DOX), shRNA is expressed due to the sequestering of TetR protein. DOX, doxycycline; GlobinIVS-TetR, GlobinIVS-Tet repressor fusion, H1, H1 promoter; hPGK, constitutive polymerase II hPGK promoter; IRES, internal ribosomal entry site; LTR, long terminal repeats; PUR, puromycin resistance gene; TATA, TATA box; TetR, Tet repressor; TRE, Tet-responsive element. Modified from Wiederschain et al. (2009) with permission from Taylor & Francis.

2.2 Cell viability assay

Cells were seeded in triplicate at densities between 250 to 3000 cells per well in 96-well plates (Corning #353072). After cells had attached, growth media were removed and replaced with drug-containing media. Following six days of treatment, cell viability was measured after incubation with 10 µg/mL resazurin (Sigma-Aldrich #R7017) for 2 hours (h) at 37˚C and 5% CO_2. In viable cells, the blue dye resazurin is converted to red fluorescent resofurin by enzymatic activity in the mitochondria. Fluorescent resofurin was measured using a plate reader (POLARstar Omega, BMG Labtech) at 544 nm. Prism software (GraphPad) was

used to analyse data. Viability of cells was expressed relative to untreated cells of the same cell line.

2.3 RNAi transfection

DLD1 (8 x 10^5) or H1299 (3 x 10^5) cells were seeded in 6 cm dishes (Greiner Bio-One #628160), before cells were reverse-transfected using Dharmafect 1 (Dharmacon #T-2001) according to manufacturer's instructions. First, 5 µL of Dharmafect reagent was added to 0.5 mL of Opti-MEM reduced serum media (Thermo Fisher Scientific #31985062) and incubated at room temperature (RT) for 5 min. Secondly, this solution was mixed with 40 nM of small interfering RNA (siRNA) in 0.5 mL Opti-MEM reduced serum media, followed by a 20-min incubation at RT and addition to the cell suspension. Media were replaced after 24 h. Immunoblotting was used to determine depletion of proteins of interest 48 h after transfection. In this study, we used the following siRNAs: GSK3α, GSK3β (Thermo Fisher Scientific #4390824; s6238 and s6241 respectively), GSK3α/β (Cell Signaling #6301) and β-catenin (Dharmacon; AUC AAC UGG AUA GUC AGC ACC).

2.4 Proliferation assay

Proteins of interest were depleted as described above, before DLD1 or H1299 cells were seeded at a density of 500 to 2000 cells per well in 96-well plates. Proliferation rate was assessed using resazurin every two days for either six days (DLD1) or eight days (H1299). Data were analysed using Excel (Microsoft) and Prism software. Population doublings were calculated relatively to day zero measurements using the following equation: Population doubling $= \log_2 \frac{\text{day x}}{\text{day 0}}$.

2.5 Drug treatment

Compounds used in this study are listed in Table 1.

Table 1: Compounds used in this study.

Name	Target	Solvent	IC_{50}	Concentration	Supplier
AZD1080	GSK3	DMSO	31 nM	0.3-10 µM	Selleckchem (#S7145)
CHIR99021	GSK3	DMSO	10 nM	0.3-10 µM	Selleckchem (#S1263)
LY2090314	GSK3	DMSO	1.5 nM	0.15-5 µM 15-500 nM	Selleckchem (#S7063)
SB216763	GSK3	DMSO	34.3 nM	0.15-5 µM	Selleckchem (#S1075)
Olaparib	PARP1/2	DMSO	5 nM	0.3-10 µM	Selleckchem (#S1060)

The *in vitro* IC_{50} values stated in Table 1 were provided by the manufacturer of the compounds. It is likely that the IC_{50} values determined *in vitro* are not sufficient to inhibit the respective target in cellular assays, where cell permeability of the compounds needs to be considered. Therefore, concentrations above the IC_{50} values were used in this study. However, it must be noted that off-target effects by the compounds are more likely to occur under these conditions.

2.6 Immunoblotting

Cells were harvested using trypsin and washed with PBS before cells were resuspended in appropriate amounts of SDS-PAGE loading buffer (0.16 M Tris-HCl pH 6.8, 4% SDS (National Diagnostics #EC-874), 20% glycerol (MP Biomedical #193996), 0.01% bromophenol blue (Thermo Fisher Scientific #B392-5), 100 mM DTT (Thermo Fisher Scientific #BP172-5)). Samples were

then sonicated, boiled for 10 min at 70˚C and centrifuged at 20,000 x g for 7 min. Protein absorbance was measured at a wavelength of 280 nm using a spectrophotometer. Proteins in solution absorb ultraviolet light at 280 nm because of the aromatic rings of certain amino acids, such as tryptophan. Using the Beer-Lambert Law, protein concentrations were calculated with the following equation: $c = \frac{A}{\varepsilon * L}$. Here, c is the protein concentration, A is the absorbance value measured at 280 nm, ε is the molar extinction coefficient and L the path length in centimetres. Equal protein amounts were analysed by SDS-PAGE and immunoblotting. Bis-Tris (Life Technologies #NP0302) or Tris-Acetate (Life Technologies #EA03752) gels were used in either MOPS or Tris-Acetate SDS running buffer (Life Technologies #NP0001 and #LA0041). Samples were separated at 180 V using the XCell SureLock Mini-Cell system (Thermo Fisher Scientific EI0001) and transferred onto a nitrocellulose membrane (GE Healthcare Life Sciences #10600001) using semi-dry transfer in transfer buffer (Life Technologies #NP00061) with 10% methanol. Membranes were blocked for unspecific binding sites in blocking buffer (5% dried skimmed milk in PBS-Tween (0.05% Tween 20 (Sigma-Aldrich #P7949) in PBS)) for 1 h. Next, membranes were incubated with primary antibody (diluted in 2% bovine serum albumin (BSA; Sigma-Aldrich #A7906) and 0.05% azide in PBS-Tween) overnight at 4˚C to detect protein of interest. Hereafter, membranes were washed three times in PBS-Tween for 5 min at RT, followed by incubation with secondary antibody (1:5000 times diluted in blocking buffer) for 1 h. Membranes were then washed in PBS-Tween three times for 10 min at RT. To detect proteins on X-ray films (Fujifilm #4741019289), ECL western blotting detection reagent (Thermo Fisher

Scientific #1859701, Millipore #WBKLS0100 or GE Healthcare #RPN2235V1/2) was used.

2.7 Antibodies

Antibodies used in this study for immunoblotting (IB) and immunofluorescence (IF) are summarised in Table 2 and Table 3.

Table 2: Primary antibodies used in this study.

Target, name	Host	Dilution (Purpose)	Target size (kDa)	Supplier
53BP1	Rabbit	1:5,000 (IF)	214	Novus Biologicals (#NB100-304)
β-catenin	Rabbit	1:1,000 (IB)	92	Cell Signaling (#9562S)
β-catenin phospho S33, S34, T41	Rabbit	1:1,000 (IB)	92	Cell Signaling (#9561)
BRCA2	Mouse	1:2,000 (IB)	390	Calbiochem (#OP95)
CHK1 (G-4)	Mouse	1:1,000 (IB)	56	Santa Cruz Biotechnology (#SC-8408)
CHK1 phospho S317	Rabbit	1:1,000 (IB)	56	Cell Signaling (#2344)
CHK1 phospho S345	Rabbit	1:1,000 (IB)	56	Cell Signaling (#2341)
GAPDH, 6C5	Mouse	1:30,000 (IB)	37	Novus Biologicals (#NB600-502)
GSK3α/β	Rabbit	1:1,000 (IB)	47 & 51	Cell Signaling (#5676S)
GSK3α/β phospho Y279/Y216	Rabbit	1:1,000 (IB)	47 & 51	Abcam (#AB75745)
RPA2, 9H8	Mouse	1:1,000 (IB)	29	Abcam (#AB2175)
RPA32 phospho S33	Rabbit	1:1,000 (IB)	32	Bethyl Laboratories (#A300-246A-1)
SMC1, BL308	Rabbit	1:10,000 (IB)	160	Bethyl Laboratories (#A300-055A)

Table 3: Secondary antibodies used in this study.

Name	Type	Supplier
DAR Cy3	Cy3 donkey anti-rat IgG	Jackson Immuno Research (#712-165-153)
GAM	Goat anti-mouse polyclonal IgG-HRP	Dako (#P0447)
GAM Alexa 488	Alexa Fluor 488 goat anti-mouse IgG	Invitrogen (#R37120)
GAR	Goat anti-rabbit polyclonal IgG HRP	Dako (#P0448)
GAR Alexa 546	Alexa Fluor 546 goat anti-rabbit IgG	Invitrogen (#A11035)

2.8 Immunofluorescence

Cells were washed in PBS, swollen in hypotonic solution (85.5 mM NaCl and 5 mM $MgCl_2$) for 5 min at RT to increase their fragility and fixed in 4% paraformaldehyde (Electron Microscopy Services #15710) for 10 min at RT. Next, cells were permeabilised (4% paraformaldehyde and 0.03% SDS) for 3 min at RT, washed with PBS supplemented with 0.4% Photoflo (Sigma-Aldrich #P7417) and blocked with antibody dilution buffer (1% goat serum (Sigma-Aldrich #G6767), 0.3% BSA, 0.005% Triton X-100 (Sigma-Aldrich #X100) in PBS). Incubation with primary antibody (diluted in antibody dilution buffer) was performed overnight at RT. On the next day, PBS supplemented with 0.4% Photoflo was used to wash the cells three times, followed by 1 h incubation with secondary antibody (1:400 dilution in antibody dilution buffer). Cells were then washes as described above and coverslips were dried and mounted on microscope slides using Prolong Antifade Gold supplemented with DAPI (Thermo Fisher Scientific #P36931). Slides were viewed with an inverted microscope (Leica DMI6000B) equipped with a HCX Plan-Apochromat 100x oil

objective with a variable numerical aperture of 1.4 to 0.7, used at the maximum numerical aperture. Images were acquired using a DFC350 FX R2 digital camera (Leica) with a pixel resolution of 2088 x 1560 and LAS-AF software (Leica). Acquired images were analysed blindly using ImageJ (National Institutes of Health, USA). The contrast of representative images was adjusted and images were cropped using Photoshop (Adobe).

2.9 DNA fibre assay

To label replicated DNA, 25 µM 5-chloro-2'-deoxyuridine (CldU; Sigma-Aldrich #C6891) was added to the media and incubated for 30 min, before cells were washed with warm PBS and followed by 30-min incubation with 250 µM 5-iodo-2'-deoxyuridine (IdU; Sigma-Aldrich #I7125). Next, cells were detached using trypsin and 5 x 10^5 cells were resuspended in ice-cold PBS. Two µL of cell suspension were incubated on a microscopy slide for 2 min, before 7 µL of lysis buffer (200 mM Tris-HCl pH 7.4, 50 mM EDTA (Sigma-Aldrich #E9884), 0.5% SDS) were added to the cell suspension and incubated for another 5 min at RT. Microscopy slides were then tilted at an angle of 30˚ - 45˚ to spread DNA. DNA was air-dried and fixed in 3:1 mixture of methanol-acetic acid (VWR #20103.330) for 10 min at RT. DNA was rehydrated in PBS twice for 3 min and denatured in 2.5 M HCl (VWR #20252.244) for 1 h at RT. Five washes with PBS for 3 min each were used to bring the pH back to neutral. Slides were then incubated with blocking buffer (2% BSA, 0.1% Tween 20, PBS; 0.22 µm filtered) for 40 min at RT. Primary antibodies (rat anti-CldU, 1:500 (Abcam #AB6326) and mouse anti-IdU, 1:100 (Becton Dickinson #347580)) were diluted in blocking buffer and added for 2.5 h at RT. Slides were washed five times for 3 min with PBS-Tween

(0.2% Tween 20 in PBS) followed by a brief wash in blocking buffer. Secondary antibodies (anti-rat Cy3, 1:300 (Jackson Immuno Research #712-165-153) and anti-mouse Alexa 488, 1:300 (Invitrogen #R37120)) were diluted in blocking buffer and added for 1 h at RT. Slides were washed five times for 3 min with PBS-Tween and air-dried. Prolong Antifade Gold (Thermo Fisher Scientific #P36930) was used to mount slides. Images were acquired and analysed as described for immunofluorescence.

2.10 Cell cycle analysis

To analyse cell cycle distribution, 5-ethynyl-2'-deoxyuridine (EdU; Thermo Fisher Scientific #A10044) was added to the media and incubated for 45 min at 37˚C to label newly synthesised DNA. Cells were then processed using the Click-iT EdU Alexa Fluor 647 Flow Cytometry Assay Kit (Thermo Fisher Scientific #C10634) according to manufacturer's instructions. In brief, cells were harvested using trypsin and washed in PBS supplemented with 1% BSA. Cells were then fixed in 4% paraformaldehyde in PBS for 15 min at RT. Subsequently, samples were washed as before and resuspended in 100 µL saponin-based permeabilisation. Next, 100 µL Click-iT reaction, containing copper, fluorescent dye azide and reaction buffer additive in PBS, were added and cells were incubated for 30 min in the dark at RT. Saponin-based permeabilisation was then used to wash cells. Cells were resuspended in PBS containing 20 µg/mL propidium iodide (Sigma-Aldrich #P4864) and 10 µg/mL RNase A (Sigma-Aldrich #R6513). Cells were processed using flow cytometry (FACSCalibur, Becton Dickinson). Cell cycle distribution was analysed using CellQuest Pro (Becton Dickinson) and FlowJo software.

2.11 Statistical analysis

Statistical differences were calculated using Prism 6 (Graphpad). *p*-values lower than 0.05 were considered statistically significant. Levels of statistical significance are expressed as follows: *, $p < 0.05$; **, $p < 0.01$; ***, $p < 0.001$; ****, $p < 0.0001$.

3 Results

3.1 Inhibition of GSK3 specifically kills HR-deficient cells

Although treatments for BRCA2-associated tumours are improving, novel approaches are still needed to cure patients. For this reason, a chemical library screen was performed in BRCA2-proficient and -deficient VC-8 hamster cells that identified GSK3 inhibitors as one of the top hits (Tacconi, 2015). VC-8 hamster cells were used as they were the only available eukaryotic BRCA2-deficient cell line with a proficient counterpart at the time.

As the chemical library screen was performed in hamster cells, we sought to validate the results in human cells. Therefore, we used BRCA2-proficient and -deficient human colorectal adenocarcinoma DLD1 cells and assessed their viability using resazurin after six days of treatment with GSK3 inhibitors LY2090314 (LY) and SB216763.

Immunoblotting confirmed the BRCA2 status of BRCA2-proficient and -deficient DLD1 cell lines (Figure 3.1A). Another way to confirm BRCA2 deficiency is to treat cells with PARP inhibitor olaparib (Bryant et al., 2005). Whilst viability of BRCA2-proficient cells was unaffected, we found that BRCA2-deficient DLD1 cells were sensitive to olaparib (Figure 3.1B), verifying that these cells lack HR capacity. In line with the outcome of the chemical library screen, we found a decrease in viability of BRCA2-deficient DLD1 cells upon GSK3 inhibition by LY or SB216763 compared to BRCA2-proficient cells (Figure 3.1C, D).

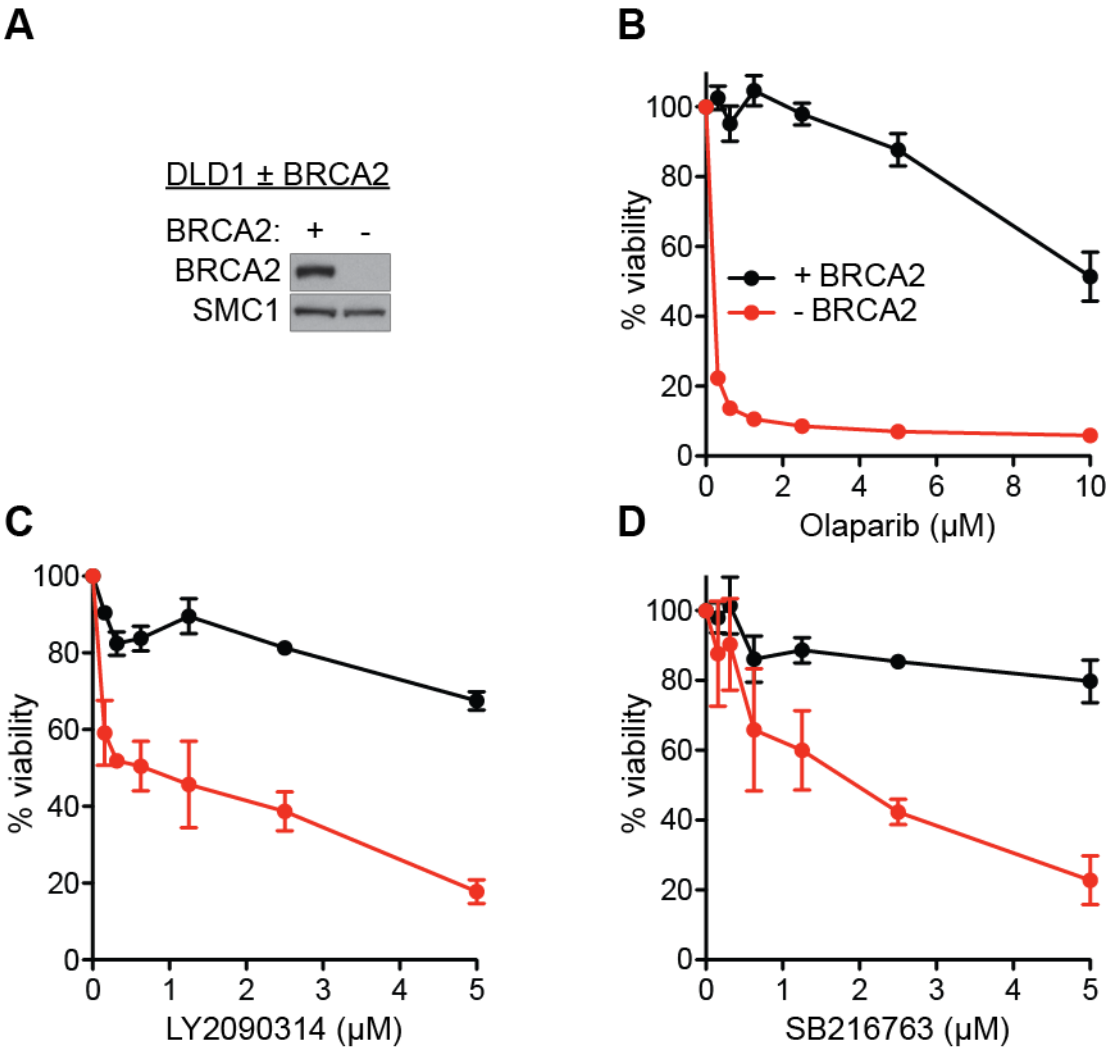

Figure 3.1. Inhibition of GSK3 leads to selectively killing of BRCA2-deficient DLD1 cells.
(**A**) Human DLD1 cells (± BRCA2) were processed for immunoblotting when treatments were initiated. SMC1 was used as a loading control. (**B**, **C** and **D**) Human DLD1 (± BRCA2) cells were incubated with the indicated concentrations of olaparib (**B**), LY2090314 (**C**) or SB216763 (**D**) for six days before processed for dose-dependent resazurin-based viability assays. Graphs shown are representative of three independent experiments, each performed in triplicate. Error bars represent SD of triplicate values obtained from a single experiment. Data shown in this figure were acquired during my Bachelor studies for Hogeschool Leiden, the Netherlands, in 2015.

To confirm these findings, we treated human H1299 cells harbouring DOX-inducible shRNA against BRCA2 with GSK3 inhibitors LY and CHIR99021 for six days before assessing cell viability using resazurin. BRCA2 depletion by addition of DOX was confirmed using immunoblotting (Figure 3.2A). In addition, H1299 cells lacking BRCA2 were sensitive to olaparib (Figure 3.2B). Interestingly, when

we compared viability of BRCA2-deficient cells to their proficient counterpart after six days of treatment with different GSK3 inhibitors, we found that cells lacking BRCA2 were more sensitive to the inhibition of GSK3 (Figure 3.2C, D).

Overall, these results are consistent with the outcome of the chemical library screen and support the idea that BRCA2-deficient cells can be targeted with GSK3 inhibitors.

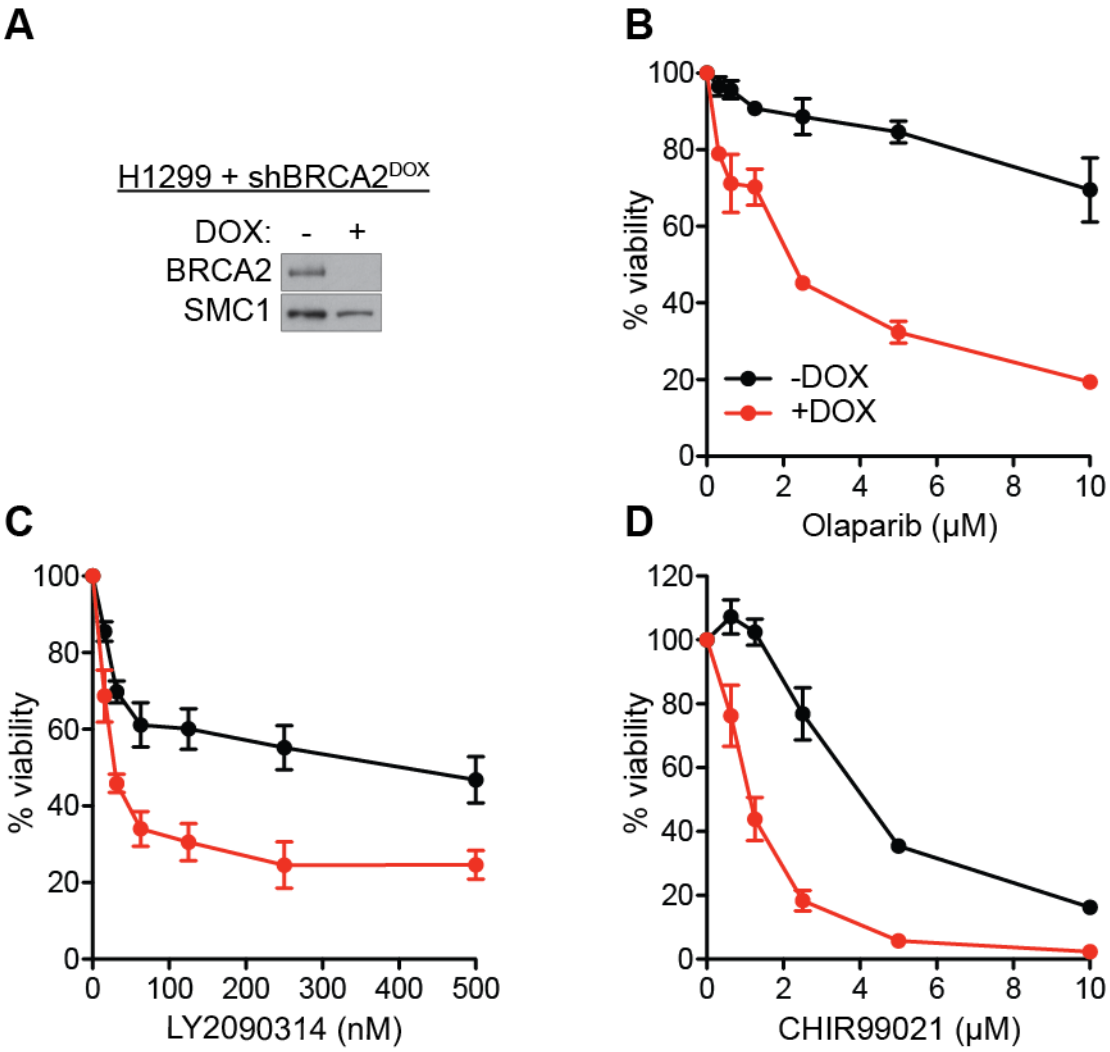

Figure 3.2. BRCA2-deficient H1299 cells are sensitive to GSK3 inhibition.
(**A**) Human H1299 cells were grown in the presence or absence of DOX for three days, before cell extracts were processed for immunoblotting. SMC1 was used as a loading control. (**B**, **C** and **D**) Human H1299 cells were treated with the indicated concentrations of olaparib (**B**), LY2090314 (**C**) or CHIR99021 (**D**). Viability was measured using resazurin after six days of treatment. Graphs shown are representative of two independent experiments, each performed in triplicate. Error bars represent SD of triplicate values obtained from a single experiment. Data shown in this figure were acquired during my Bachelor studies for Hogeschool Leiden, the Netherlands, in 2015. DOX, doxycycline.

3.2 Depletion of GSK3 is synthetic lethal with BRCA2 abrogation

The *GSK3α and GSK3β* genes encode the two proteins of the serine/threonine kinase GSK3 (Plyte et al., 1992; Woodgett, 1990). Importantly, inhibitors that target GSK3 bind to both GSK3α and GSK3β (Meijer et al., 2004). To investigate whether GSK3α or GSK3β needs to be suppressed to reduce the viability of

BRCA2-deficient cells, we monitored the proliferation rate of BRCA2-proficient and -deficient DLD1 cells depleted in GSK3α, GSK3β or both. Resazurin-based proliferation assays were used to assess population doublings every 48 h.

Immunoblotting established specific RNAi-mediated depletion of the respective GSK3 protein (Figure 3.3A). We found that neither GSK3α nor GSK3β depletion affected the proliferation rates of BRCA2-proficient or -deficient DLD1 cells (Figure 3.3B, C). When we depleted both GSK3α and GSK3β, we observed a mild decrease in the proliferation rate of BRCA2-proficient cells. Remarkably, cells lacking BRCA2 failed to proliferate when GSK3α and GSK3β were depleted (Figure 3.3D).

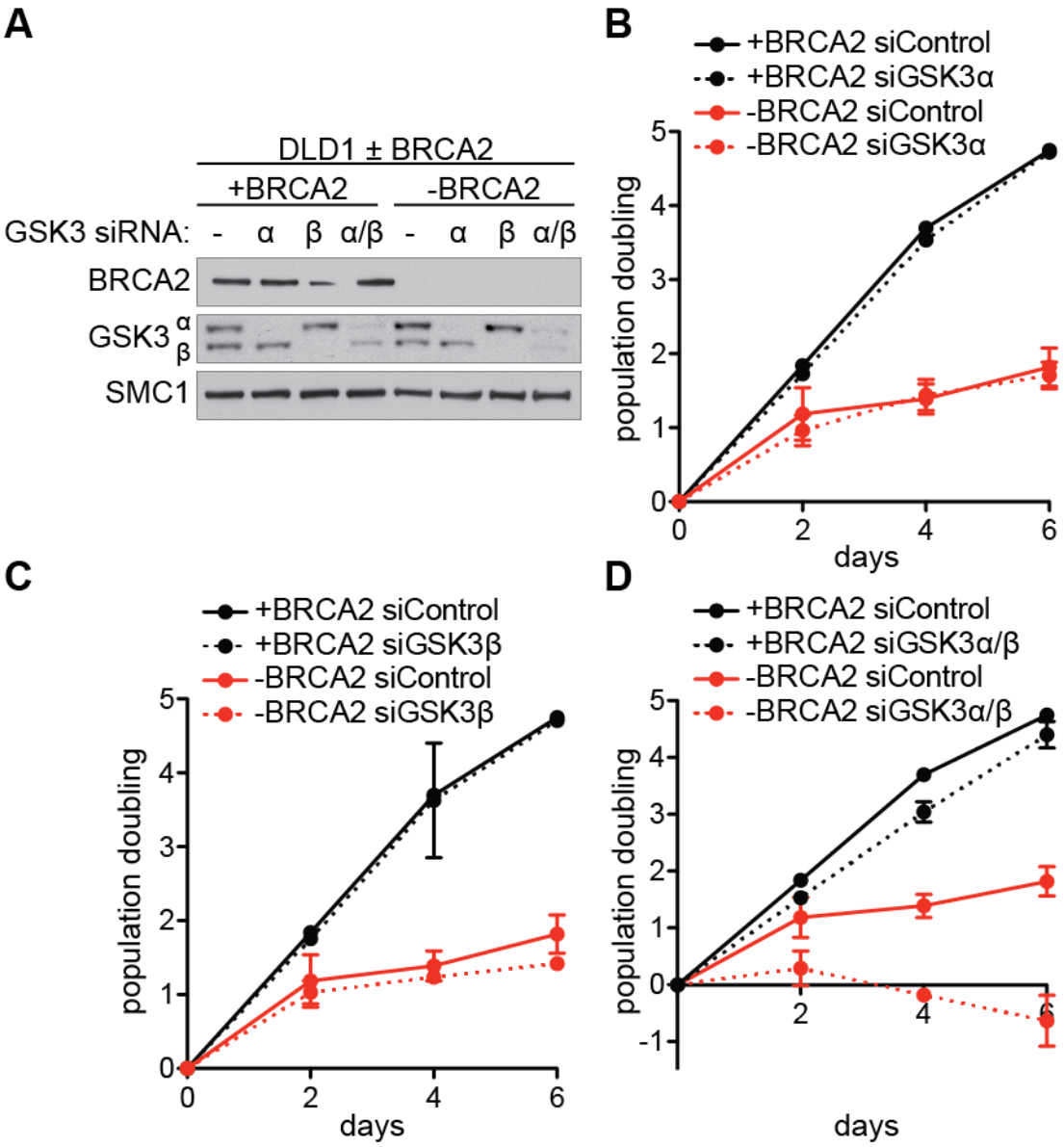

Figure 3.3. Depletion of GSK3 is synthetic lethal with BRCA2 abrogation in DLD1 cells.
Human DLD1 cells were transfected with a non-targeting, GSK3α, GSK3β or GSK3α/β siRNA. (**A**) After 48 h of incubation with siRNA, extracts were processed for immunoblotting to check depletions. SMC1 was used as a loading control. (**B**, **C** and **D**) Population doubling was measured using resazurin every 2 days for 6 days of GSK3α (**B**), GSK3β (**C**) and GSK3α/β (**D**) depleted cells. Graphs shown are obtained from a single experiment, performed in triplicate. Error bars represent SD of triplicate values.

We obtained similar results in H1299 cells, in which BRCA2 depletion was mediated by DOX-inducible shRNA and GSK3α, GSK3β or both were depleted using RNAi (Figure 3.4A). No proliferation decrease was observed when GSK3α or GSK3β was depleted in BRCA2-proficient or -deficient H1299 cells (Figure

3.4B, C). Nonetheless, we found that H1299 cells lacking BRCA2 hardly proliferated when expression of both GSK3α and GSK3β was abrogated (Figure 3.4D).

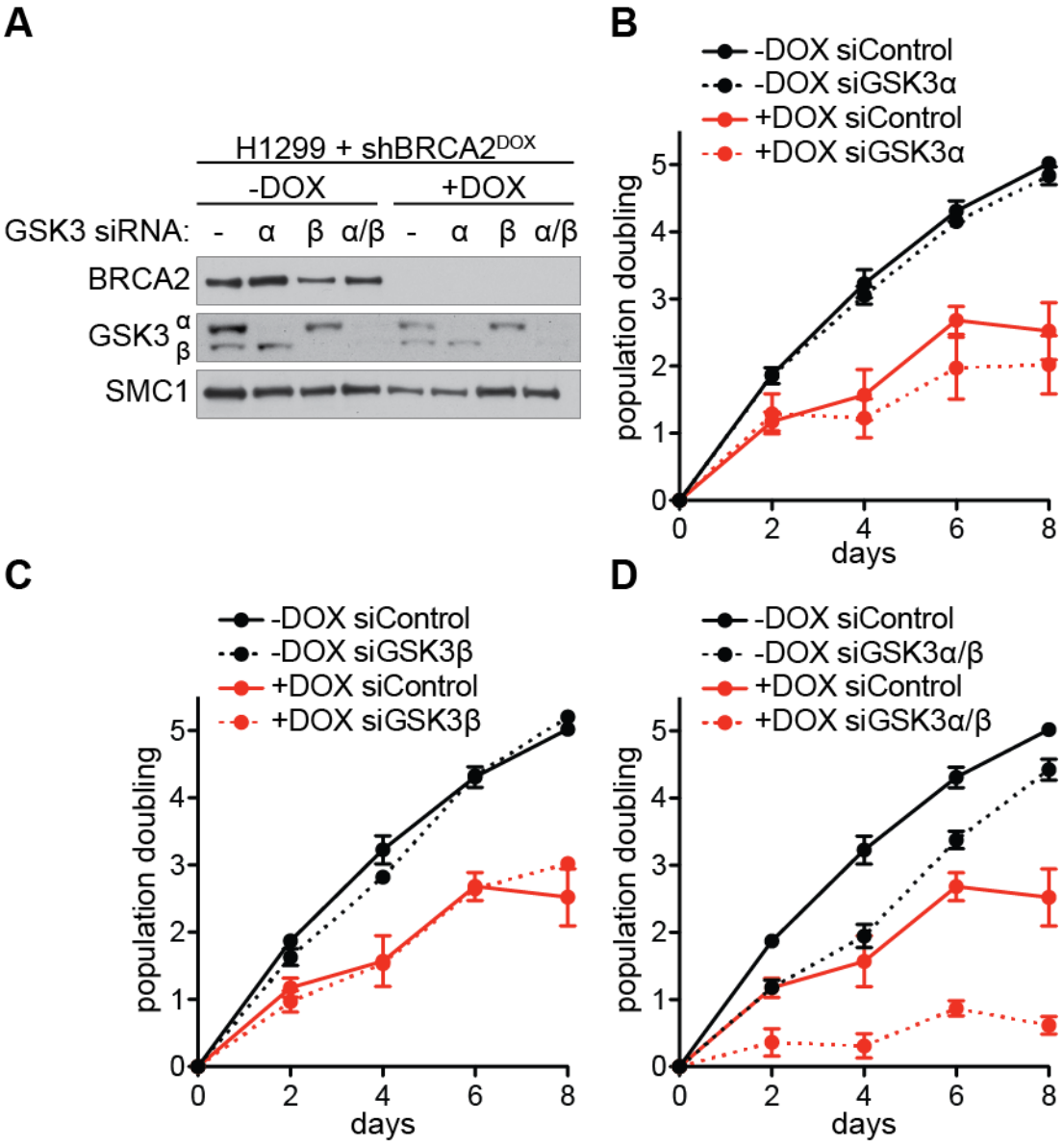

Figure 3.4. Synthetic lethal interaction between GSK3 and BRCA2 in H1299 cells. Human H1299 cells were grown in the presence or absence of DOX for three days, before cells were transfected with a non-targeting, GSK3α, GSK3β or GSK3α/β siRNA. (**A**) After 48 h of incubation with siRNA, extracts were processed for immunoblotting to check depletions. SMC1 was used as a loading control. (**B**, **C** and **D**) Population doubling was measured using resazurin every 2 days for 8 days of GSK3α (**B**), GSK3β (**C**) and GSK3α/β (**D**) depleted cells. Graphs shown are representative of two independent experiments, each performed in triplicate. Error bars represent SD of triplicate values obtained from a single experiment. DOX, doxycycline.

In summary, we found that depletion of either GSK3α or GSK3β alone is not synthetic lethal with BRCA2 abrogation, indicating that one of the GSK3 proteins can compensate for the loss of the other. However, simultaneous depletion of GSK3α and GSK3β is lethal in BRCA2-deficient cells. These results are in line with the results observed with the chemical inhibitors, which inhibit both GSK3α and GSK3β, and indicate that HR-defective cells rely on GSK3 activity.

3.3 GSK3 inhibition causes replication stress

Recently, a study showed that cancer cells overexpressing the oncogene *HRAS* accumulate replication stress, DNA damage and genome instability caused by upregulation of transcription activity (Kotsantis et al., 2016). Furthermore, multiple studies have demonstrated that stabilised β-catenin acts as an activator of transcription and that the accumulation of β-catenin leads to the oncogenic activation of the protein (Anastas et al., 2013; Morin et al., 1997; Polakis, 1999; Rubinfeld et al., 1997). Thus, we hypothesised that GSK3 inhibition-mediated β-catenin accumulation may cause replication stress, similarly to *HRAS* overexpression.

To test our hypothesis, BRCA2-proficient and -deficient H1299 cells were processed for immunoblotting after treatment with the GSK3 inhibitor LY for one, two or three days (Figure 3.5A). Lack of phosphorylation at Y279 on GSK3α and at Y216 on GSK3β was indicative of efficient GSK3 inhibition (Figure 3.5A). Consistently, proteasome-targeting phosphorylation of β-catenin was abolished and β-catenin was stabilised upon GSK3 inhibition (Figure 3.5A). Upon replication stress, ATR kinase phosphorylates ssDNA-binding protein RPA on S33 to facilitate fork recovery. Therefore, phosphorylation of RPA on S33 is

commonly used as an indicative of replication stress (Zeman et al., 2014; Zou et al., 2003a). Interestingly, we found an induction of phospho (p)-RPA on S33 after LY-mediated GSK3 inhibition (Figure 3.5A).

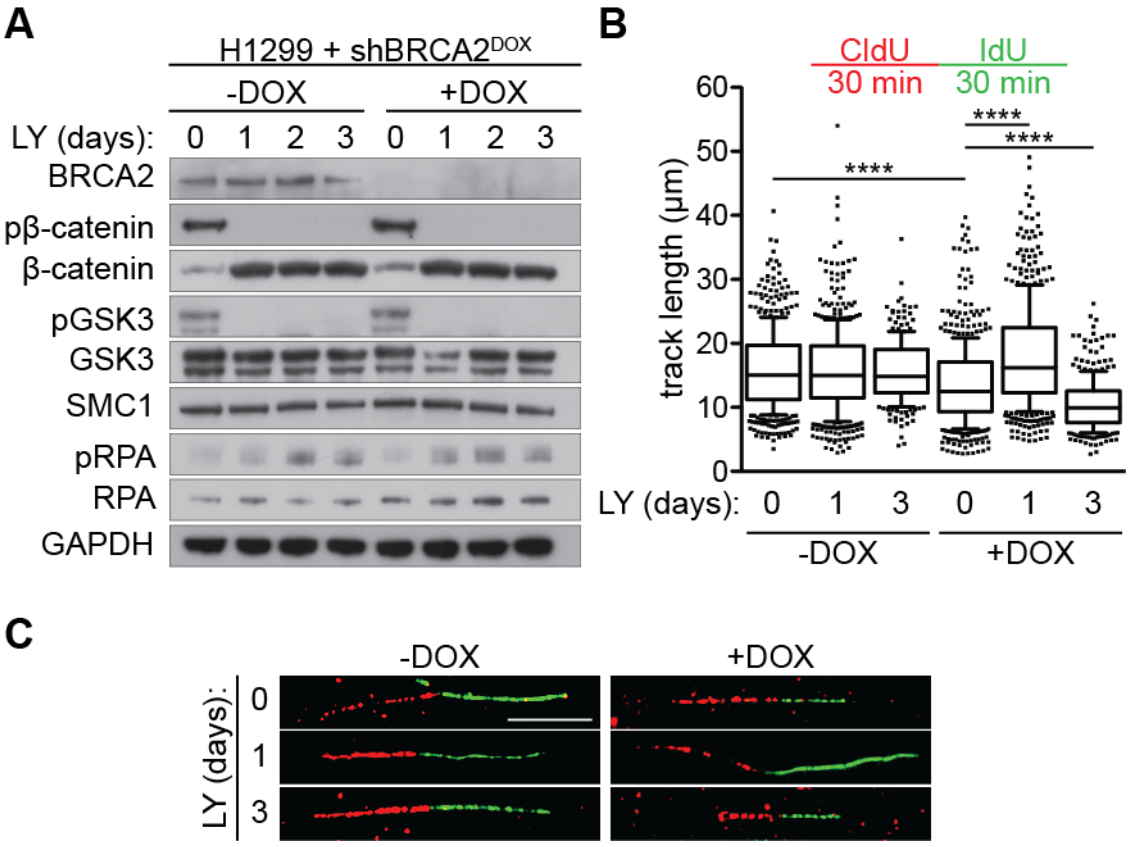

Figure 3.5. GSK3 inhibition leads to β-catenin accumulation and induces replication stress.
(**A**) Human H1299 cells were grown in the presence or absence of DOX for three days, before cells were treated as indicated with 250 nM LY2090314 and prepared for immunoblotting. SMC1 and GAPDH were used as loading controls. Immunoblot shown is representative of two independent experiments. (**B**) Quantification of fibre track length of H1299 cells treated as indicated with 250 nM LY2090314. Middle line represents median, and the box extends from the 25th to 75th percentiles. The whiskers mark the 10th and 90th percentiles. Each dot represents one fibre. At least 100 fibres were quantified per condition and experiment. n = 3 for 0 and 1 day treatment; n = 2 for 3 days of treatment. ****, $p < 0.0001$ (two-tailed Mann-Whitney test). (**C**) Representative images of fibres treated as in (**B**). Scale bar, 10 µm; DOX, doxycycline; LY, LY2090314; p, phospho; min, minutes.

Replication stress can be visualised more directly using the DNA fibre technique, which is based on the incorporation of thymidine analogues CldU and IdU

(Bianco et al., 2012). We treated BRCA2-proficient and -deficient H1299 cells for either one or three days with GSK3 inhibitor LY before replicated DNA was labelled with CldU and IdU. Total track length was quantified as a readout for the rate of DNA synthesis.

Whilst the replication track length of BRCA2-proficient cells remained unaffected, we detected a significant increase in the track length of BRCA2-deficient cells after one day of LY treatment (Figure 3.5B, C). Strikingly, a marked decrease in the track length of BRCA2-deficient cells was observed after three days of GSK3 inhibition (Figure 3.5B, C).

Overall, accumulation of pRPA and altered replication dynamics indicate that the inhibition of GSK3 leads to replication stress.

3.4 Inhibition of GSK3 leads to DSBs and genome instability

It has been suggested that replication stress can lead to DNA damage (Zeman et al., 2014). Therefore, we stained BRCA2-proficient and -deficient H1299 with the DSB marker 53BP1 to monitor DNA damage accumulation after GSK3 inhibition using immunofluorescence. Foci were counted manually and cells with more than 10 53BP1 foci were considered as DNA damage-positive. It must be noted that there are limitations to quantifying foci manually. Firstly, overlapping foci may not visible and, secondly, the intensity and size of foci are not considered.

BRCA2-proficient H1299 did not accumulate 53BP1 foci after one or three days of LY-mediated GSK3 inhibition (Figure 3.6A, C). Interestingly, we found a significant increase in the percentage of BRCA2-deficient cells with 10 or more

53BP1 foci after treatment (Figure 3.6A, C). These results indicate that GSK3 inhibition leads to DSB formation specifically in cells lacking BRCA2.

Micronuclei are commonly used as a readout for genome instability (Fenech et al., 2011). Errors during mitosis can lead to lagging chromosomes, which often result in micronuclei (Thompson et al., 2011). In contrast to BRCA2-proficient cells, we found a robust increase in cells with micronuclei after three days of GSK3 inhibition in cells lacking BRCA2 (Figure 3.6B, C). This suggests that inhibition of GSK3 leads to mitotic errors in the context of BRCA2 deficiency.

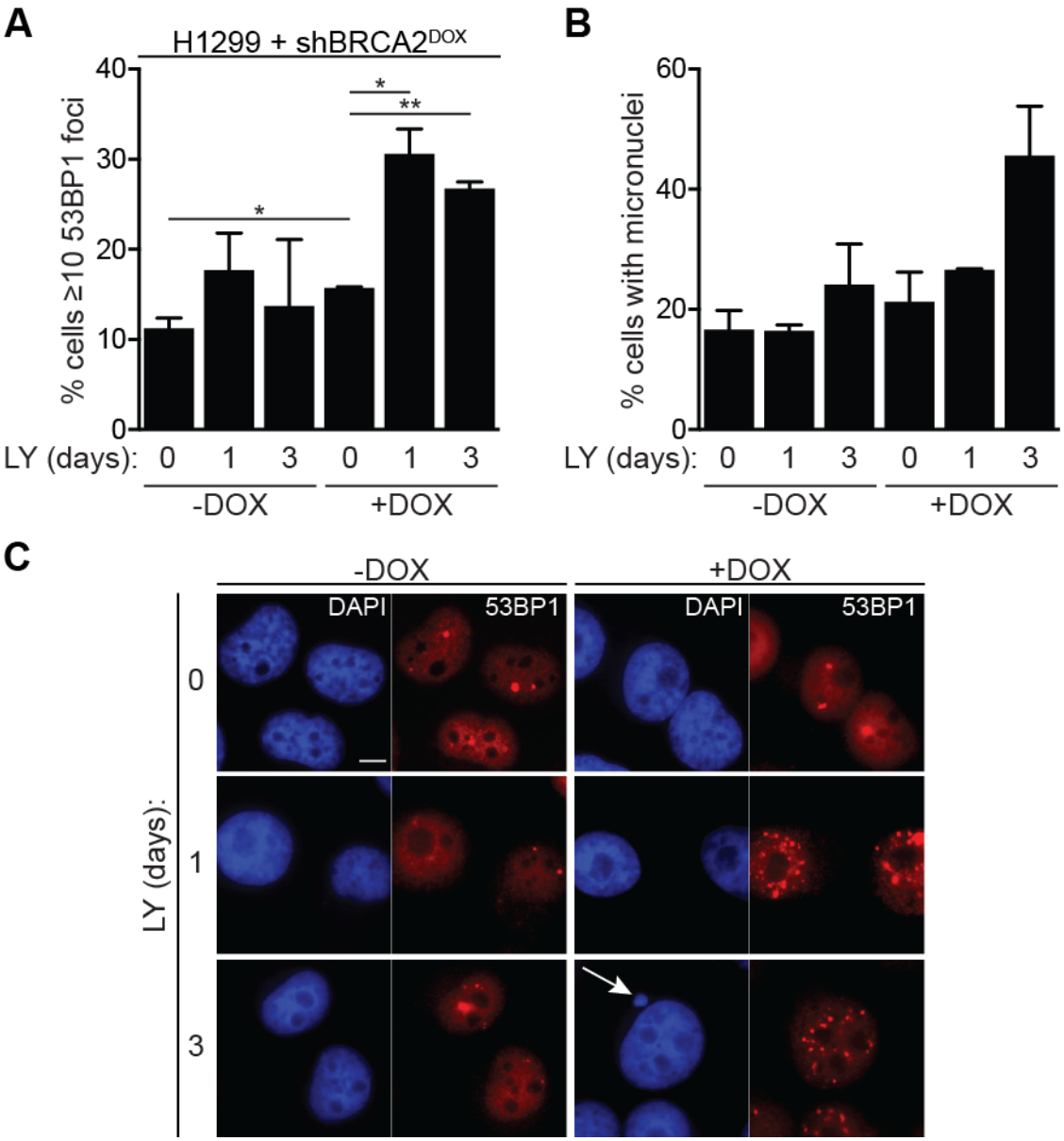

Figure 3.6. Chemical inhibition of GSK3 triggers DNA damage and genome instability.
Human H1299 cells were grown in the presence or absence of DOX for three days, before cells were treated as indicated with 250 nM LY2090314 and prepared for immunofluorescence staining with 53BP1 antibody. (**A**) Quantification of the frequency of cells with ≥10 53BP1 foci. $n = 2$; error bars, SD. * $p < 0.05$; ** $p < 0.01$ (unpaired two-tailed t test). (**B**) Quantification of percentage of cells with micronuclei. At least 100 cells were analyses per condition and experiment. $n = 2$; error bars, SD. (**C**) Representative images of cells treated as in (**A**). Arrow indicates micronuclei; scale bar 10 µm; DOX, doxycycline; LY, LY2090314.

3.5 Lethality induced by GSK3 inhibition is β-catenin depended

We have shown that inhibition of GSK3 leads to replication stress and genome instability specifically in cells defective in HR through loss of BRCA2 expression.

However, it remained unclear how the silencing of GSK3 caused these phenotypes. Given that simultaneous depletion of GSK3α and GSK3β was lethal in BRCA2-deficient cells (Figure 3.3D and Figure 3.4D) and that both proteins are required for the regulation of β-catenin (Doble et al., 2007), we set out to investigate the role of β-catenin in this context. More specifically, we sought to address whether the accumulation of β-catenin, caused by the inhibition of GSK3 (Figure 3.5A), was toxic to BRCA2-deficient cells.

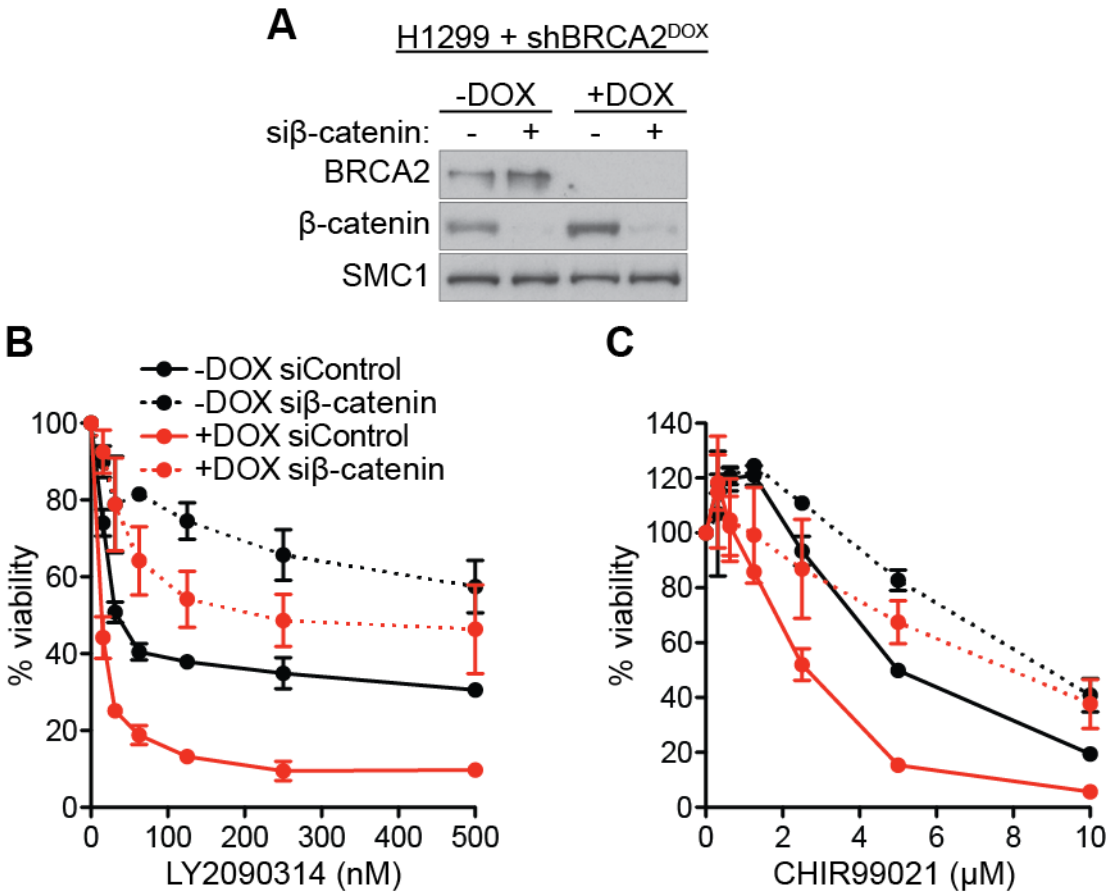

Figure 3.7. Depletion of β-catenin rescues lethality induced by GSK3 inhibition. Human H1299 cells were grown in the presence or absence of DOX for three days, before cells were transfected with a non-targeting or β-catenin siRNA. (**A**) After 48 h of incubation with siRNA, extracts were processed for immunoblotting to check depletion. SMC1 was used as a loading control. (**B** and **C**) Cells were incubated with the indicating concentrations of LY2090314 (**B**) or CHIR99021 (**C**) for six days before processing for dose-dependent viability assays. Graphs shown are representative of three independent experiments, each preformed in triplicate. Error bars represent SD of triplicate values obtained from a single experiment. DOX, doxycycline; si, siRNA.

To prevent the stabilisation of β-catenin, we depleted β-catenin using RNAi, before we treated the cells with two different GSK3 inhibitors (LY and CHIR99021) in resazurin-based viability assays. Depletion of β-catenin was confirmed using immunoblotting (Figure 3.7A). Similar to our previous results (Figure 3.2C, D), we observed a marked reduction in the viability of BRCA2-deficient H1299 cells compared to their proficient counterparts, after six days of treatment with either GSK3 inhibitor (Figure 3.7B, C). Strikingly, viability of both BRCA2-proficient and -deficient H1299 cells was rescued in cells depleted in β-catenin upon LY- or CHIR99021-mediated GSK3 inhibition (Figure 3.7B, C).

These results suggest that the accumulation of β-catenin by GSK3 inhibition may cause the decrease in cell viability.

3.6 Accumulation of β-catenin causes replication stress

Next, we investigated whether the replication stress induced by GSK3 inhibition (Figure 3.5) was mediated by β-catenin accumulation. Therefore, β-catenin was silenced using RNAi in BRCA2-proficient and -deficient H1299 cells followed by treatment with GSK3 inhibitor LY for one or three days and immunoblotting.

Lack of the activating phosphorylation sites Y279 on GSK3α and Y216 on GSK3β, after LY treatment, confirmed efficient GSK3 inhibition (Figure 3.8). In addition, phosphorylation of β-catenin on S33, S37 and T41 was abrogated after GSK3 inhibition, indicating that β-catenin was not targeted for degradation by the proteasome. Accordingly, total levels of β-catenin were increased upon treatment with LY compared to the untreated controls. However, β-catenin stabilisation was only observed in cells transfected with control siRNA (Figure 3.8 lanes 1-3 and 7-9) and not in cells depleted in β-catenin (Figure 3.8 lanes 4-6 and 10-12).

Overall, these results confirmed the efficient inhibition of GSK3 and silencing of β-catenin by RNAi.

To explore whether β-catenin stabilisation triggered replication stress, we investigated the phosphorylation of ssDNA-binding protein RPA. We found an increase in phosphorylation of RPA on S33 specifically in cells deficient in BRCA2, transfected with control siRNA (Figure 3.8 lanes 7-9). Strikingly, in cells lacking both BRCA2 and β-catenin, we found a reduction in pRPA after GSK3 inhibition (Figure 3.8 lanes 10-12) compared to cells lacking only BRCA2 (Figure 3.8 lanes 7-9). This indicates that GSK3 inhibition-mediated β-catenin accumulation causes replication stress.

RPA accumulation on ssDNA leads to ATR activation, which triggers checkpoint activation (Liu et al., 2000; Melo et al., 2002; Zhao et al., 2001; Zou et al., 2003a). To explore whether GSK3 inhibition led to checkpoint activation mediated by β-catenin accumulation, we assessed phosphorylation of CHK1 on S317 and S345. Accumulation of pCHK1 was observed upon treatment with GSK3 inhibitor LY, which was more pronounced in the cells lacking BRCA2 (Figure 3.8 compare lanes 1-3 with 7-9). Interestingly, lower levels of pCHK1 were found in cells deficient in BRCA2 and β-catenin (Figure 3.8 compare lanes 7-9 with 10-12), indicating that checkpoint activation in response to GSK3 inhibition was at least partially caused by β-catenin accumulation.

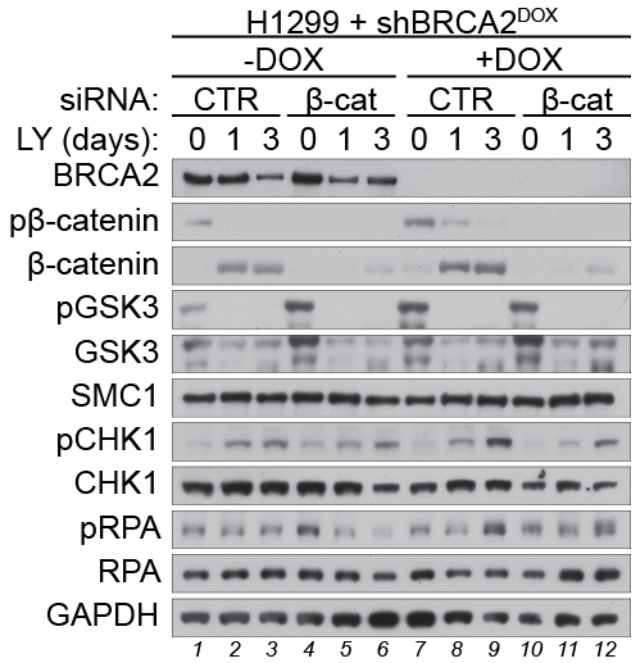

Figure 3.8. GSK3 inhibition-mediated β-catenin accumulation causes replication stress.
Human H1299 cells were grown in the presence or absence of DOX for three days, before cells were transfected with a control or β-catenin siRNA. After 48 h of incubation with siRNA, cells were treated with 250 nM LY2090314 for indicated times and processed for immunoblotting (*n* = 1). DOX, doxycycline; CTR, control; β-cat, β-catenin; LY, LY2090314; p, phospho.

Checkpoint activation can lead to cell cycle arrest (Liu et al., 2000; Melo et al., 2002; Zhao et al., 2001). Therefore, we were interested whether the observed phosphorylation of CHK1 induced cell cycle arrest and if this was dependent on β-catenin accumulation. Using RNAi, we depleted β-catenin and treated BRCA2-proficient and -deficient H1299 cells with LY for one day, followed by incubation with thymidine analogue EdU to label newly synthesised DNA. The cell cycle distribution was assessed using FACS analysis.

Untreated BRCA2-proficient and -deficient cells displayed distinct cell cycle profiles (Figure 3.9A). Approximately 30% of the total population of untreated BRCA2-proficient cells were in G1 phase compared to 60% of untreated BRCA2-deficient cells (Figure 3.9A). Interestingly, the percentage of S phase cells was significantly increased after one day of treatment with the GSK3 inhibitor, in both

BRCA2-proficient and -deficient cells (Figure 3.9B). The percentage of BRCA2-proficient cells in S phase increased from 54% in untreated cells to 61% after treatment (Figure 3.9B). In BRCA2-deficient S phase cells, an increase from 19% to 50% was observed upon GSK3 inhibition (Figure 3.9B). Interestingly, the accumulation of cells in S phase after GSK3 inhibition was prohibited by depleting β-catenin in BRCA2-proficient cells (Figure 3.9B). In BRCA2-deficient cells, however, β-catenin depletion reversed the GSK3 inhibitor-mediated rise in the percentage of S phase cells only partially (Figure 3.9B).

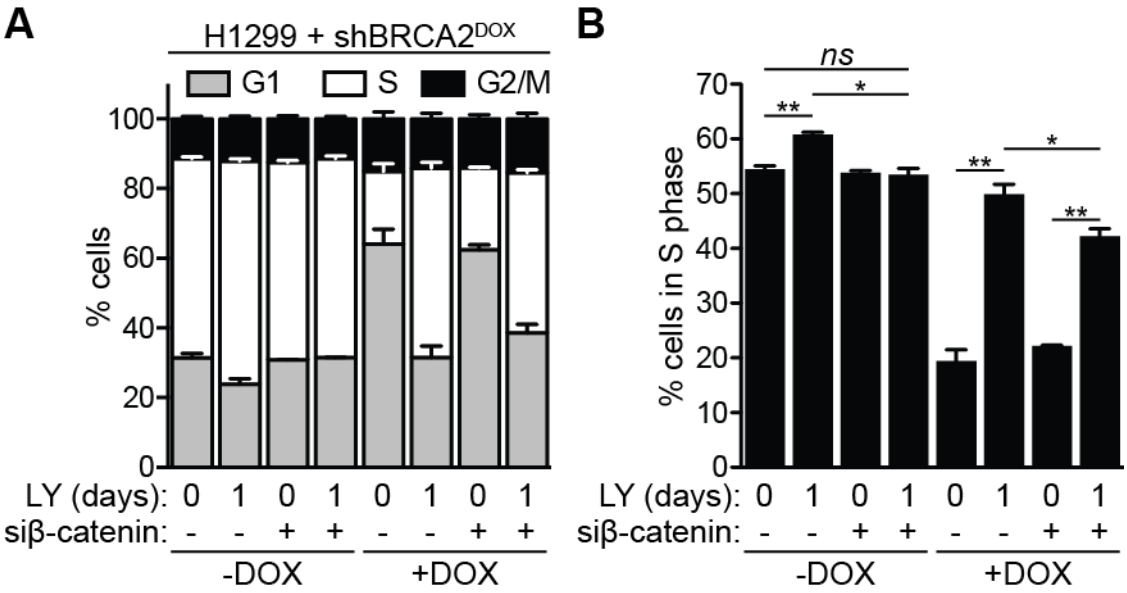

Figure 3.9. Prevention of β-catenin accumulation partially rescues S phase accumulated cells.
(**A**) Human H1299 cells were grown in the presence or absence of DOX for three days, before cells were transfected with a non-targeting or β-catenin siRNA. After 48 h of incubation with siRNA, cells were treated as indicated with 250 nM LY2090314 before cells were incubated for 45 min with EdU and processed for FACS analyses of DNA content. *n* = 2; error bars, SD (**B**) Quantification of cells in S phase of cells treated as in (**A**). *n* = 2; error bars, SD; * $p < 0.05$; ** $p < 0.01$ (unpaired two-tailed t test). At least 10,000 cells were analyses per condition and experiment. DOX, doxycycline; LY, LY2090314; *ns*, not significant; si, siRNA.

In summary, these results indicate that accumulation of β-catenin through GSK3 inhibition triggers replication stress and checkpoint activation. In addition,

inhibition of GSK3 leads to an accumulation of cells in S phase in both BRCA2-proficient and -deficient, which is partially mediated by β-catenin stabilisation.

3.7 Olaparib-resistant *Brca1*-deficient cells exhibit sensitivity to GSK3 inhibition

A common problem with HR-associated tumours is that patients acquire resistance against currently used therapies. One mechanism, by which *Brca1*-deficient tumour cells can gain resistance against PARP inhibitors, is mediated by the loss of 53BP1 (Bouwman et al., 2010; Bunting et al., 2010; Cao et al., 2009). It is believed that cells lacking both BRCA1 and 53BP1 are able to reactive HR activity by restoring resection at the DSB (Bunting et al., 2010).

To assess whether cells that have acquired resistance against PARP inhibitor olaparib were sensitive to GSK3 inhibition, we used mouse mammary tumour cells that were *wild type* (*Brca1*$^{+/+}$), *Brca1*$^{-/-}$ or *Brca1*$^{-/-}$ and 53BP1-deficient. Resistance to olaparib of *Brca1*$^{-/-}$, 53BP1-deficient mouse cells was confirmed in a viability assay, where *Brca1*$^{-/-}$ cells were sensitive to PARP inhibition and *wild type* cells remained unaffected (Figure 3.10A). Interestingly, viability of both PARP-sensitive (*Brca1*$^{-/-}$) and -resistant (*Brca1*$^{-/-}$, 53BP1-deficient) cells was decreased after treatment with GSK3 inhibitor AZD1080, whilst *wildtype* (*Brca1*$^{+/+}$) cells remained viable (Figure 3.10B).

These results imply that GSK3 inhibitor may be effective to treat BRCA1-deficient tumours that have acquired resistance against PARP inhibitors.

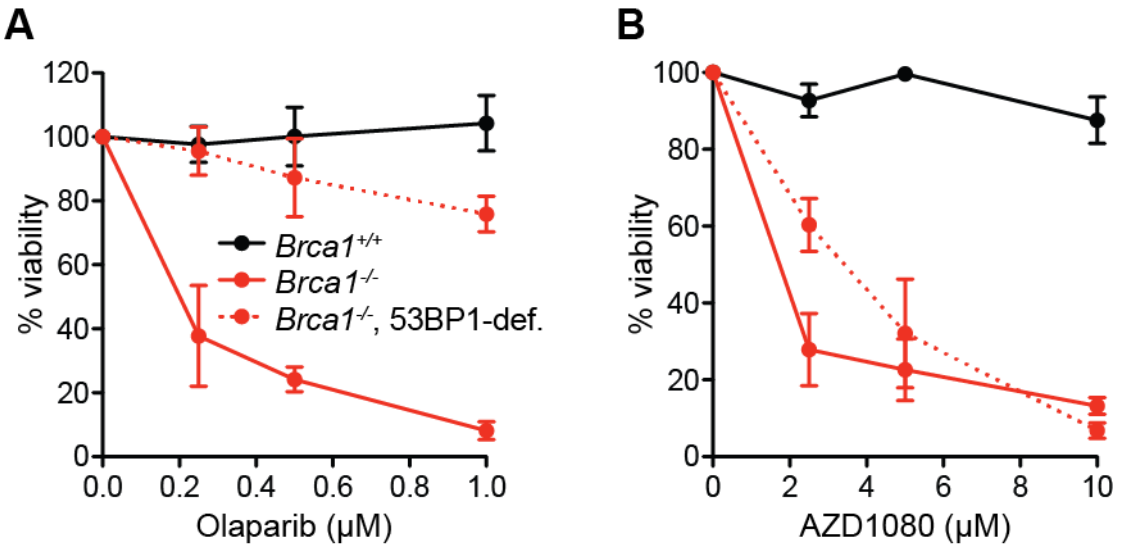

Figure 3.10. Olaparib-resistant mouse tumour-derived cells are sensitive to GSK3 inhibition.

Mouse mammary tumour-derived cell lines were treated with the indicated concentrations of olaparib (**A**) or AZD1080 (**B**) for six days before processing for dose-dependent viability assays. Graphs shown are representative of three independent experiments, each preformed in triplicate. Error bars represent SD of triplicate values obtained from a single experiment. def., deficient.

4 Discussion

Despite continuous improvements in the treatment of cancer, the cure rates of BRCA-associated tumours remain low. GSK3 inhibitors were identified as a potent tool to kill BRCA2-deficient cells in a chemical library screen (Tacconi, 2015). In this study, we sought to characterise GSK3 inhibitors as a novel means to target BRCA2 deficiency.

Chemical and genetic approaches for inhibition of GSK3 reduced the viability of BRCA2-deficient DLD1 and H1299 cells (Figure 3.1, Figure 3.2, Figure 3.3 and Figure 3.4), confirming the outcome of the chemical library screen. A higher concentration of the GSK3 inhibitor LY was used in DLD1 cells compared to the H1299 cells, up to 5 μM in contrast to 500 nM, respectively (Figure 3.1C and Figure 3.2C). It is important to note that DLD1 cells harbour a mutation in *APC*, leading to elevated levels of β-catenin (Tang et al., 2008). Interestingly, DLD1 cells accumulate β-catenin when treated with GSK3 inhibitor LY (Zonderland, 2016). However, due to the mutation in *APC*, silencing of β-catenin is lethal in DLD1 cells (Hwang et al., 2016), regardless of BRCA2 status. This led us to focus on the characterisation of GSK3 inhibitors in the context of BRCA2 deficiency in H1299 cells.

Serine/threonine kinase GSK3 plays a central role in the WNT pathway, in which the inactivation of GSK3 leads to the stabilisation of β-catenin (Figure 1.3). Treatment with the GSK3 inhibitor LY confirmed efficient silencing of its target using immunoblotting. Phosphorylation of GSK3α on Y279 and GSK3β on Y216, which mediates activation, was abrogated after treatment, and β-catenin was stabilised (Figure 3.5A). Moreover, phosphorylation of β-catenin on S33, S37 and

T41 was abolished upon GSK3 inhibition (Figure 3.5A). Overall, this confirmed activation of the WNT pathway by GSK3 inhibition.

Multiple studies have argued that oncogene activation can lead to replication stress, often referred to as oncogene-induced replication stress (Di Micco et al., 2006; Gorgoulis et al., 2010; Halazonetis et al., 2008; Hills et al., 2014; Kotsantis et al., 2016; Murga et al., 2011). Accordingly, we hypothesised that β-catenin accumulation may lead to its oncogenic activation and therefore cause replication stress. Indeed, RPA phosphorylation on S33 was increased in cells treated with LY (Figure 3.5A). Furthermore, we observed a longer track length after one day of GSK3 inhibition, specifically in BRCA2-deficient cells (Figure 3.5B, C). Remarkably, the track length in cells lacking BRCA2 was shorter after three days of treatment (Figure 3.5B, C). One explanation for this phenotype may be that β-catenin induces cell proliferation, which can lead to uncontrolled replication. This can in turn induce DNA damage, which has to be repaired and therefore replication slows down. Consistently, we observed an increase in 53BP1 foci upon GSK3 inhibition specifically in BRCA2-defective cells (Figure 3.6A, C). Additionally, only in cells lacking BRCA2 treated for three days with LY, we observed an enhanced percentage of cells with micronuclei (Figure 3.6B, C). This suggests that GSK3 inhibition leads to DNA damage and mitotic defects in BRCA2-deficient cells.

To investigate β-catenin's role in the killing of BRCA2-deficient cells upon GSK3 inhibition, we prevented its accumulation using RNAi and treated the cells in resazurin-based viability assays with two different GSK3 inhibitors (Figure 3.7). Remarkably, we found that cells lacking β-catenin were less sensitive for GSK3 inhibition than cells proficient in β-catenin (Figure 3.7), indicating that β-catenin

accumulation upon GSK3 inhibition decreases cell viability. To further test whether GSK3 inhibition-mediated β-catenin accumulation causes replication stress, we monitored phosphorylation of RPA on S33 after GSK3 inhibition in cells depleted in β-catenin. Whilst BRCA2-deficient cells exhibited a robust increase of pRPA upon GSK3 inhibition compared to untreated cells, cells lacking both BRCA2 and β-catenin did not display this increase (Figure 3.8). Accordingly, checkpoint activation was delayed in cells simultaneously depleted for BRCA2 and β-catenin, in contrast to cells lacking only BRCA2 (Figure 3.8). These results support our hypothesis that β-catenin accumulation caused by GSK3 inhibition leads to replication stress. Furthermore, inhibition of GSK3 led to an increase of percentage of cells in S phase, a phenotype that was only partially mediated by β-catenin (Figure 3.9).

Cells lacking BRCA1 can acquire resistance against currently used therapies. BRCA1-deficient cells lacking 53BP1 expression are able to reactivate HR by restoration of resection (Bunting et al., 2010). Strikingly, we found that *Brca1*-, 53BP1-deficient cells, resistant for PARP inhibitor olaparib, were sensitive to GSK3 inhibition (Figure 3.10). However, further mechanistic insight is needed to understand the underlying mechanism of the sensitivity to the GSK3 inhibitor. Previously, ATR inhibitors and a G-quadruplex stabiliser have been shown to kill olaparib-resistant cells due to failure to load at DSB sites (Yazinski et al., 2017; Zimmer et al., 2016). Therefore, it would be interesting to test whether RAD51 is loaded at break sites in *Brca1*-, 53BP1-deficient cells treated with the GSK3 inhibitor. If not, this could provide an explanation why olaparib-resistant cells remain sensitive to GSK3 inhibition.

Given that GSK3 regulates many proteins and pathways, it has been debated whether targeting GSK3 therapeutically is a clinically relevant approach (Rayasam et al., 2009). However, treatment of bipolar mood disorder patients with GSK3 inhibitor lithium did not increase the risk for developing cancer (Cohen et al., 2004; Cohen et al., 1998). In addition to lithium, other GSK3 inhibitors have been tested to treat a range of diseases, including cancer (McCubrey et al., 2014). For example, GSK3 inhibitor LY was used in a clinical trial for metastatic pancreatic cancer (ClinicalTrial.gov identifier: NCT01632306). This supports the notion that GSK3 inhibitors can be used therapeutically. However, long-term treatments and further trials are necessary to address the clinical potential of GSK3 inhibitors in cancer and especially in a BRCA-deficient context.

Future work is required to gain a better understanding of the mechanism, by which GSK3 inhibition leads to selectively elimination of BRCA-deficient cells. It will be important to test whether the inhibition of GSK3 causes mitotic defects, given that BRCA2 is involved in the mitotic spindle checkpoint (Choi et al., 2012). In addition, GSK3 and β-catenin are required for accurate centrosome separation (Bahmanyar et al., 2008; Kaplan et al., 2004; Yoshino et al., 2015). Therefore, it is possible that the inhibition of GSK3 causes incorrect centrosome separation leading to mitotic defects. This can lead to genome instability in cells without a functional spindle checkpoint and thereby induce selective killing of BRCA2-deficient cells (Figure 4.1A, B).

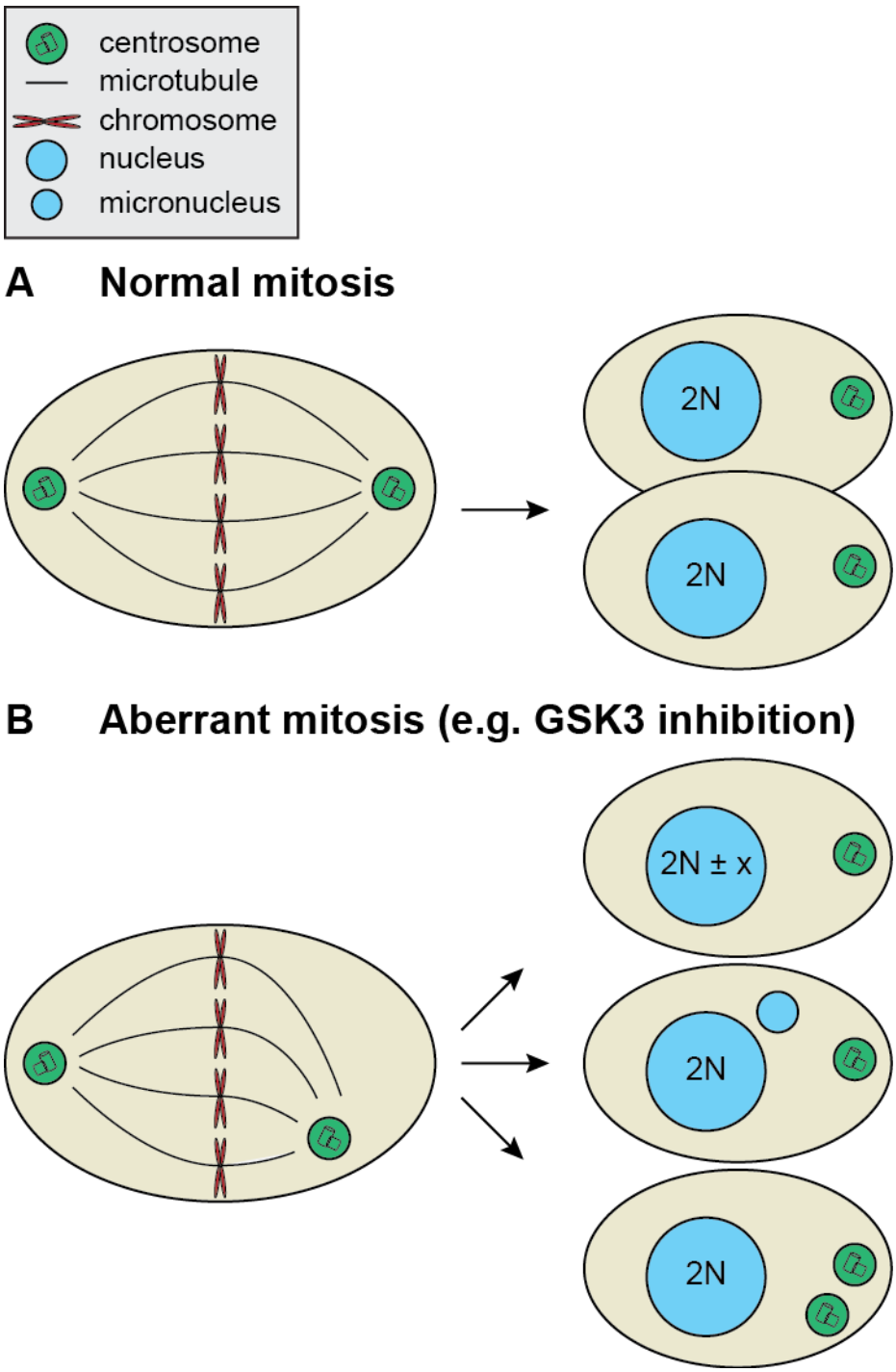

Figure 4.1. Model for GSK3 inhibition-induced genome instability.
A model that potentially explains the synthetic lethal interaction between BRCA2 and GSK3. (**A**) During mitosis chromosomes are separated accurately by two centrosomes, resulting in two identical daughter cells. (**B**) In the context of GSK3 inhibition, centrosomes are separated inaccurately, leading to chromosome missegregation. This can result in the formation of micronuclei, aneuploidy or multiple centrosomes in the daughter cell. Due to the role of BRCA2 in the mitotic spindle checkpoint, mitosis can be blocked and genomic instability in the daughter cell is prevented.

Another option is that the inhibition of GSK3 leads to elevated levels of transcription activity. Newly formed RNA can bind to the ssDNA generated by DNA replication, causing RNA:DNA hybrid formation (Daniels et al., 1995; Reaban et al., 1990; Reaban et al., 1994). These RNA:DNA hybrids cannot be repaired efficiently in the absence of BRCA2 (Bhatia et al., 2014). In addition to RNA:DNA hybrids, elevation of transcription activity can trigger collision of the transcription machinery and a replication fork, leading to fork stalling (Aguilera, 2002). Therefore, an increase of transcription activity can be a source of genome instability (Figure 4.2A, B) (Kotsantis et al., 2016). These two hypotheses that may explain the selectively killing of BRCA-deficient cells by GSK3 inhibitors will require further experimental evidence.

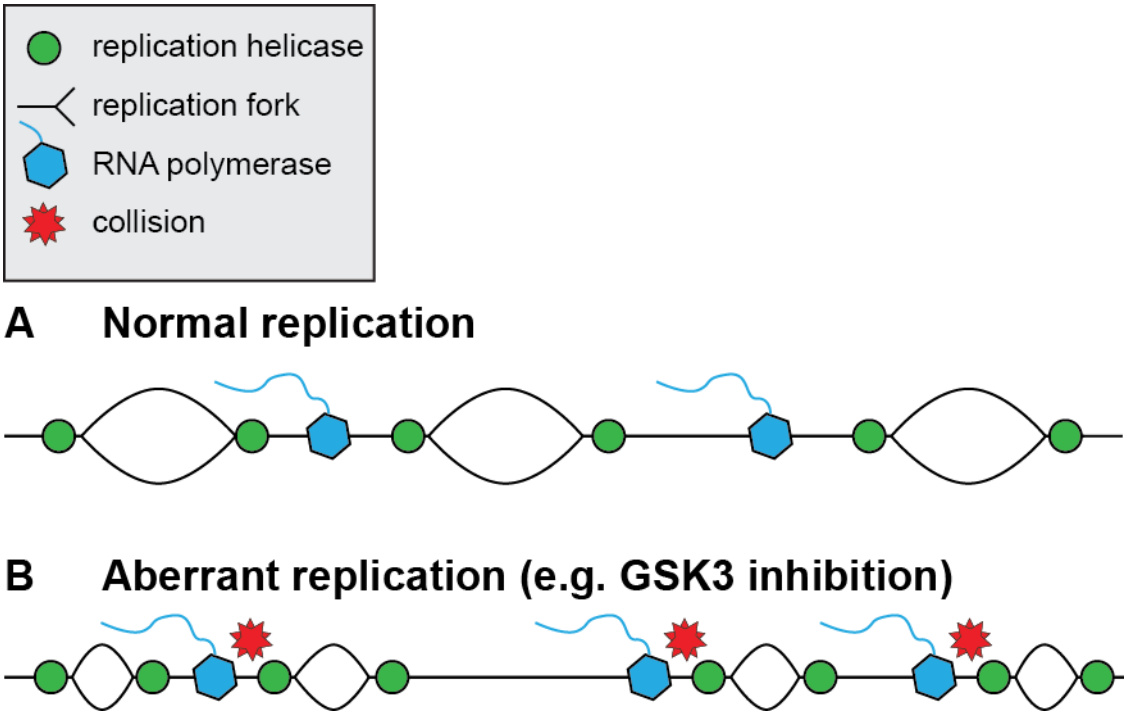

Figure 4.2. Model for GSK3 inhibition-induced replication stress.
Second potential model that may explain the sensitivity of BRCA2-deficient cells to GSK3 inhibitors. (**A**) During S phase, replication forks and RNA polymerases are tightly regulated to prevent collisions between the two. (**B**) In this model, we propose that inhibition of GSK3 leads to the accumulation of β-catenin, which acts as a transcription activator. As a result, transcription activities are increases and replication forks slow down. This can lead to the collision of RNA polymerases and replication forks, which causes DSBs. Due to the role of BRCA2 in repairing DBSs, this is lethal in BRCA2-deficient cells.

Conclusion

Here, we show that the inhibition of GSK3 is toxic to human cells lacking BRCA2. This study indicates that the sensitivity of BRCA2-deficient cells to GSK3 inhibition stems from replication stress and DNA damage. In addition, mouse cells resistant to PARP inhibitor olaparib are susceptible to GSK3 inhibition. Overall, this study highlights the potential of GSK3 inhibitors to abrogate BRCA-deficient cell survival.

5 References

Aguilera, A. 2002. The connection between transcription and genomic instability. *EMBO J*. 21:195-201.

Ahnesorg, P., P. Smith, and S.P. Jackson. 2006. XLF interacts with the XRCC4-DNA ligase IV complex to promote DNA nonhomologous end-joining. *Cell*. 124:301-313.

Amit, S., A. Hatzubai, Y. Birman, J.S. Andersen, E. Ben-Shushan, M. Mann, Y. Ben-Neriah, and I. Alkalay. 2002. Axin-mediated CKI phosphorylation of beta-catenin at Ser 45: a molecular switch for the Wnt pathway. *Genes Dev*. 16:1066-1076.

Anastas, J.N., and R.T. Moon. 2013. WNT signalling pathways as therapeutic targets in cancer. *Nat Rev Cancer*. 13:11-26.

Arnaudeau, C., C. Lundin, and T. Helleday. 2001. DNA double-strand breaks associated with replication forks are predominantly repaired by homologous recombination involving an exchange mechanism in mammalian cells. *J Mol Biol*. 307:1235-1245.

Audeh, M.W., J. Carmichael, R.T. Penson, M. Friedlander, B. Powell, K.M. Bell-McGuinn, C. Scott, J.N. Weitzel, A. Oaknin, N. Loman, K. Lu, R.K. Schmutzler, U. Matulonis, M. Wickens, and A. Tutt. 2010. Oral poly(ADP-ribose) polymerase inhibitor olaparib in patients with BRCA1 or BRCA2 mutations and recurrent ovarian cancer: a proof-of-concept trial. *Lancet*. 376:245-251.

Bahmanyar, S., D.D. Kaplan, J.G. Deluca, T.H. Giddings, Jr., E.T. O'Toole, M. Winey, E.D. Salmon, P.J. Casey, W.J. Nelson, and A.I. Barth. 2008. beta-Catenin is a Nek2 substrate involved in centrosome separation. *Genes Dev*. 22:91-105.

Barber, L.J., S. Sandhu, L. Chen, J. Campbell, I. Kozarewa, K. Fenwick, I. Assiotis, D.N. Rodrigues, J.S. Reis Filho, V. Moreno, J. Mateo, L.R. Molife, J. De Bono, S. Kaye, C.J. Lord, and A. Ashworth. 2013. Secondary mutations in BRCA2 associated with clinical resistance to a PARP inhibitor. *J Pathol*. 229:422-429.

Baumann, P., F.E. Benson, and S.C. West. 1996. Human Rad51 protein promotes ATP-dependent homologous pairing and strand transfer reactions in vitro. *Cell*. 87:757-766.

Bhatia, V., S.I. Barroso, M.L. Garcia-Rubio, E. Tumini, E. Herrera-Moyano, and A. Aguilera. 2014. BRCA2 prevents R-loop accumulation and associates with TREX-2 mRNA export factor PCID2. *Nature*. 511:362-365.

Bianco, J.N., J. Poli, J. Saksouk, J. Bacal, M.J. Silva, K. Yoshida, Y.L. Lin, H. Tourriere, A. Lengronne, and P. Pasero. 2012. Analysis of DNA replication profiles in budding yeast and mammalian cells using DNA combing. *Methods*. 57:149-157.

Boddy, M.N., P.H. Gaillard, W.H. McDonald, P. Shanahan, J.R. Yates, 3rd, and P. Russell. 2001. Mus81-Eme1 are essential components of a Holliday junction resolvase. *Cell*. 107:537-548.

Boersma, V., N. Moatti, S. Segura-Bayona, M.H. Peuscher, J. van der Torre, B.A. Wevers, A. Orthwein, D. Durocher, and J.J. Jacobs. 2015. MAD2L2 controls DNA repair at telomeres and DNA breaks by inhibiting 5' end resection. *Nature*. 521:537-540.

Bothmer, A., D.F. Robbiani, N. Feldhahn, A. Gazumyan, A. Nussenzweig, and M.C. Nussenzweig. 2010. 53BP1 regulates DNA resection and the choice between classical and alternative end joining during class switch recombination. *J Exp Med*. 207:855-865.

Bouwman, P., A. Aly, J.M. Escandell, M. Pieterse, J. Bartkova, H. van der Gulden, S. Hiddingh, M. Thanasoula, A. Kulkarni, Q. Yang, B.G. Haffty, J. Tommiska, C. Blomqvist, R. Drapkin, D.J. Adams, H. Nevanlinna, J. Bartek, M. Tarsounas, S. Ganesan, and J. Jonkers. 2010. 53BP1 loss rescues BRCA1 deficiency and is associated with triple-negative and BRCA-mutated breast cancers. *Nat Struct Mol Biol*. 17:688-695.

Bryant, H.E., N. Schultz, H.D. Thomas, K.M. Parker, D. Flower, E. Lopez, S. Kyle, M. Meuth, N.J. Curtin, and T. Helleday. 2005. Specific killing of BRCA2-deficient tumours with inhibitors of poly(ADP-ribose) polymerase. *Nature*. 434:913-917.

Buisson, R., J. Niraj, A. Rodrigue, C.K. Ho, J. Kreuzer, T.K. Foo, E.J. Hardy, G. Dellaire, W. Haas, B. Xia, J.Y. Masson, and L. Zou. 2017. Coupling of Homologous Recombination and the Checkpoint by ATR. *Mol Cell*. 65:336-346.

Bunting, S.F., E. Callen, N. Wong, H.T. Chen, F. Polato, A. Gunn, A. Bothmer, N. Feldhahn, O. Fernandez-Capetillo, L. Cao, X. Xu, C.X. Deng, T. Finkel, M. Nussenzweig, J.M. Stark, and A. Nussenzweig. 2010. 53BP1 inhibits homologous recombination in Brca1-deficient cells by blocking resection of DNA breaks. *Cell*. 141:243-254.

Byun, T.S., M. Pacek, M.C. Yee, J.C. Walter, and K.A. Cimprich. 2005. Functional uncoupling of MCM helicase and DNA polymerase activities activates the ATR-dependent checkpoint. *Genes Dev*. 19:1040-1052.

Cao, L., X. Xu, S.F. Bunting, J. Liu, R.H. Wang, L.L. Cao, J.J. Wu, T.N. Peng, J. Chen, A. Nussenzweig, C.X. Deng, and T. Finkel. 2009. A selective requirement for 53BP1 in the biological response to genomic instability induced by Brca1 deficiency. *Mol Cell*. 35:534-541.

Chen, H., M. Lisby, and L.S. Symington. 2013. RPA coordinates DNA end resection and prevents formation of DNA hairpins. *Mol Cell*. 50:589-600.

Choi, E., P.G. Park, H.O. Lee, Y.K. Lee, G.H. Kang, J.W. Lee, W. Han, H.C. Lee, D.Y. Noh, S. Lekomtsev, and H. Lee. 2012. BRCA2 fine-tunes the spindle assembly checkpoint through reinforcement of BubR1 acetylation. *Dev Cell*. 22:295-308.

Cobb, J.A., L. Bjergbaek, K. Shimada, C. Frei, and S.M. Gasser. 2003. DNA polymerase stabilization at stalled replication forks requires Mec1 and the RecQ helicase Sgs1. *EMBO J*. 22:4325-4336.

Cohen, P., and M. Goedert. 2004. GSK3 inhibitors: development and therapeutic potential. *Nat Rev Drug Discov*. 3:479-487.

Cohen, Y., A. Chetrit, Y. Cohen, P. Sirota, and B. Modan. 1998. Cancer morbidity in psychiatric patients: influence of lithium carbonate treatment. *Med Oncol*. 15:32-36.

Cole, A., S. Frame, and P. Cohen. 2004. Further evidence that the tyrosine phosphorylation of glycogen synthase kinase-3 (GSK3) in mammalian cells is an autophosphorylation event. *Biochem J*. 377:249-255.

Cross, D.A., D.R. Alessi, P. Cohen, M. Andjelkovich, and B.A. Hemmings. 1995. Inhibition of glycogen synthase kinase-3 by insulin mediated by protein kinase B. *Nature*. 378:785-789.

Cross, D.A., D.R. Alessi, J.R. Vandenheede, H.E. McDowell, H.S. Hundal, and P. Cohen. 1994. The inhibition of glycogen synthase kinase-3 by insulin or insulin-like growth factor 1 in the rat skeletal muscle cell line L6 is blocked by wortmannin, but not by rapamycin: evidence that wortmannin blocks activation of the mitogen-activated protein kinase pathway in L6 cells between Ras and Raf. *Biochem J*. 303 (Pt 1):21-26.

Daniels, G.A., and M.R. Lieber. 1995. RNA:DNA complex formation upon transcription of immunoglobulin switch regions: implications for the mechanism and regulation of class switch recombination. *Nucleic Acids Res*. 23:5006-5011.

De Piccoli, G., Y. Katou, T. Itoh, R. Nakato, K. Shirahige, and K. Labib. 2012. Replisome stability at defective DNA replication forks is independent of S phase checkpoint kinases. *Mol Cell*. 45:696-704.

Di Micco, R., M. Fumagalli, A. Cicalese, S. Piccinin, P. Gasparini, C. Luise, C. Schurra, M. Garre, P.G. Nuciforo, A. Bensimon, R. Maestro, P.G. Pelicci, and F. d'Adda di Fagagna. 2006. Oncogene-induced senescence is a DNA damage response triggered by DNA hyper-replication. *Nature*. 444:638-642.

Ding, X., A. Ray Chaudhuri, E. Callen, Y. Pang, K. Biswas, K.D. Klarmann, B.K. Martin, S. Burkett, L. Cleveland, S. Stauffer, T. Sullivan, A. Dewan, H. Marks, A.T. Tubbs, N. Wong, E. Buehler, K. Akagi, S.E. Martin, J.R. Keller, A. Nussenzweig, and S.K. Sharan. 2016. Synthetic viability by BRCA2 and PARP1/ARTD1 deficiencies. *Nat Commun*. 7:12425.

Doble, B.W., S. Patel, G.A. Wood, L.K. Kockeritz, and J.R. Woodgett. 2007. Functional redundancy of GSK-3alpha and GSK-3beta in Wnt/beta-catenin signaling shown by using an allelic series of embryonic stem cell lines. *Dev Cell*. 12:957-971.

Dobzhansky, T. 1946. Genetics of Natural Populations. Xiii. Recombination and Variability in Populations of Drosophila Pseudoobscura. *Genetics*. 31:269-290.

Dominguez, I., K. Itoh, and S.Y. Sokol. 1995. Role of glycogen synthase kinase 3 beta as a negative regulator of dorsoventral axis formation in Xenopus embryos. *Proc Natl Acad Sci U S A*. 92:8498-8502.

Edwards, S.L., R. Brough, C.J. Lord, R. Natrajan, R. Vatcheva, D.A. Levine, J. Boyd, J.S. Reis-Filho, and A. Ashworth. 2008. Resistance to therapy caused by intragenic deletion in BRCA2. *Nature*. 451:1111-1115.

Eldar-Finkelman, H., and A. Martinez. 2011. GSK-3 Inhibitors: Preclinical and Clinical Focus on CNS. *Front Mol Neurosci*. 4:32.

Embi, N., D.B. Rylatt, and P. Cohen. 1980. Glycogen synthase kinase-3 from rabbit skeletal muscle. Separation from cyclic-AMP-dependent protein kinase and phosphorylase kinase. *Eur J Biochem*. 107:519-527.

Farmer, H., N. McCabe, C.J. Lord, A.N. Tutt, D.A. Johnson, T.B. Richardson, M. Santarosa, K.J. Dillon, I. Hickson, C. Knights, N.M. Martin, S.P. Jackson, G.C. Smith, and A. Ashworth. 2005. Targeting the DNA repair defect in BRCA mutant cells as a therapeutic strategy. *Nature*. 434:917-921.

Fenech, M., M. Kirsch-Volders, A.T. Natarajan, J. Surralles, J.W. Crott, J. Parry, H. Norppa, D.A. Eastmond, J.D. Tucker, and P. Thomas. 2011. Molecular mechanisms of micronucleus, nucleoplasmic bridge and nuclear bud formation in mammalian and human cells. *Mutagenesis*. 26:125-132.

Fisher, A.E., H. Hochegger, S. Takeda, and K.W. Caldecott. 2007. Poly(ADP-ribose) polymerase 1 accelerates single-strand break repair in concert with poly(ADP-ribose) glycohydrolase. *Mol Cell Biol*. 27:5597-5605.

Fong, P.C., D.S. Boss, T.A. Yap, A. Tutt, P. Wu, M. Mergui-Roelvink, P. Mortimer, H. Swaisland, A. Lau, M.J. O'Connor, A. Ashworth, J. Carmichael, S.B. Kaye, J.H. Schellens, and J.S. de Bono. 2009. Inhibition of poly(ADP-ribose) polymerase in tumors from BRCA mutation carriers. *N Engl J Med*. 361:123-134.

Frame, S., and P. Cohen. 2001. GSK3 takes centre stage more than 20 years after its discovery. *Biochem J*. 359:1-16.

Gorgoulis, V.G., and T.D. Halazonetis. 2010. Oncogene-induced senescence: the bright and dark side of the response. *Curr Opin Cell Biol*. 22:816-827.

Grawunder, U., M. Wilm, X. Wu, P. Kulesza, T.E. Wilson, M. Mann, and M.R. Lieber. 1997. Activity of DNA ligase IV stimulated by complex formation with XRCC4 protein in mammalian cells. *Nature*. 388:492-495.

Gu, J., H. Lu, B. Tippin, N. Shimazaki, M.F. Goodman, and M.R. Lieber. 2007. XRCC4:DNA ligase IV can ligate incompatible DNA ends and can ligate across gaps. *EMBO J*. 26:1010-1023.

Haince, J.F., D. McDonald, A. Rodrigue, U. Dery, J.Y. Masson, M.J. Hendzel, and G.G. Poirier. 2008. PARP1-dependent kinetics of recruitment of MRE11 and NBS1 proteins to multiple DNA damage sites. *J Biol Chem*. 283:1197-1208.

Hakem, R., J.L. de la Pompa, C. Sirard, R. Mo, M. Woo, A. Hakem, A. Wakeham, J. Potter, A. Reitmair, F. Billia, E. Firpo, C.C. Hui, J. Roberts, J. Rossant, and T.W. Mak. 1996. The tumor suppressor gene Brca1 is required for embryonic cellular proliferation in the mouse. *Cell*. 85:1009-1023.

Halazonetis, T.D., V.G. Gorgoulis, and J. Bartek. 2008. An oncogene-induced DNA damage model for cancer development. *Science*. 319:1352-1355.

Hanada, K., M. Budzowska, M. Modesti, A. Maas, C. Wyman, J. Essers, and R. Kanaar. 2006. The structure-specific endonuclease Mus81-Eme1 promotes conversion of interstrand DNA crosslinks into double-strands breaks. *EMBO J*. 25:4921-4932.

Hanger, D.P., K. Hughes, J.R. Woodgett, J.P. Brion, and B.H. Anderton. 1992. Glycogen synthase kinase-3 induces Alzheimer's disease-like phosphorylation of tau: generation of paired helical filament epitopes and neuronal localisation of the kinase. *Neurosci Lett*. 147:58-62.

Hart, M., J.P. Concordet, I. Lassot, I. Albert, R. del los Santos, H. Durand, C. Perret, B. Rubinfeld, F. Margottin, R. Benarous, and P. Polakis. 1999. The F-box protein beta-TrCP associates with phosphorylated beta-catenin and regulates its activity in the cell. *Curr Biol*. 9:207-210.

He, T.C., A.B. Sparks, C. Rago, H. Hermeking, L. Zawel, L.T. da Costa, P.J. Morin, B. Vogelstein, and K.W. Kinzler. 1998. Identification of c-MYC as a target of the APC pathway. *Science*. 281:1509-1512.

He, X., J.P. Saint-Jeannet, J.R. Woodgett, H.E. Varmus, and I.B. Dawid. 1995. Glycogen synthase kinase-3 and dorsoventral patterning in Xenopus embryos. *Nature*. 374:617-622.

Helleday, T. 2011. The underlying mechanism for the PARP and BRCA synthetic lethality: clearing up the misunderstandings. *Mol Oncol*. 5:387-393.

Hills, S.A., and J.F. Diffley. 2014. DNA replication and oncogene-induced replicative stress. *Curr Biol*. 24:R435-444.

Hoeflich, K.P., J. Luo, E.A. Rubie, M.S. Tsao, O. Jin, and J.R. Woodgett. 2000. Requirement for glycogen synthase kinase-3beta in cell survival and NF-kappaB activation. *Nature*. 406:86-90.

Hucl, T., C. Rago, E. Gallmeier, J.R. Brody, M. Gorospe, and S.E. Kern. 2008. A syngeneic variance library for functional annotation of human variation: application to BRCA2. *Cancer Res*. 68:5023-5030.

Huertas, P., F. Cortes-Ledesma, A.A. Sartori, A. Aguilera, and S.P. Jackson. 2008. CDK targets Sae2 to control DNA-end resection and homologous recombination. *Nature*. 455:689-692.

Hwang, S.Y., X. Deng, S. Byun, C. Lee, S.J. Lee, H. Suh, J. Zhang, Q. Kang, T. Zhang, K.D. Westover, A. Mandinova, and S.W. Lee. 2016. Direct Targeting of

beta-Catenin by a Small Molecule Stimulates Proteasomal Degradation and Suppresses Oncogenic Wnt/beta-Catenin Signaling. *Cell Rep*. 16:28-36.

Jackson, S.P., and J. Bartek. 2009. The DNA-damage response in human biology and disease. *Nature*. 461:1071-1078.

Johnson, R.D., and M. Jasin. 2000. Sister chromatid gene conversion is a prominent double-strand break repair pathway in mammalian cells. *EMBO J*. 19:3398-3407.

Johnson, R.D., N. Liu, and M. Jasin. 1999. Mammalian XRCC2 promotes the repair of DNA double-strand breaks by homologous recombination. *Nature*. 401:397-399.

Kaplan, D.D., T.E. Meigs, P. Kelly, and P.J. Casey. 2004. Identification of a role for beta-catenin in the establishment of a bipolar mitotic spindle. *J Biol Chem*. 279:10829-10832.

Kawanishi, S., and M. Murata. 2006. Mechanism of DNA damage induced by bromate differs from general types of oxidative stress. *Toxicology*. 221:172-178.

King, M.C., J.H. Marks, J.B. Mandell, and G. New York Breast Cancer Study. 2003. Breast and ovarian cancer risks due to inherited mutations in BRCA1 and BRCA2. *Science*. 302:643-646.

Kitagawa, M., S. Hatakeyama, M. Shirane, M. Matsumoto, N. Ishida, K. Hattori, I. Nakamichi, A. Kikuchi, K. Nakayama, and K. Nakayama. 1999. An F-box protein, FWD1, mediates ubiquitin-dependent proteolysis of beta-catenin. *EMBO J*. 18:2401-2410.

Kotsantis, P., L.M. Silva, S. Irmscher, R.M. Jones, L. Folkes, N. Gromak, and E. Petermann. 2016. Increased global transcription activity as a mechanism of replication stress in cancer. *Nat Commun*. 7:13087.

Latres, E., D.S. Chiaur, and M. Pagano. 1999. The human F box protein beta-Trcp associates with the Cul1/Skp1 complex and regulates the stability of beta-catenin. *Oncogene*. 18:849-854.

Lindahl, T., and D.E. Barnes. 2000. Repair of endogenous DNA damage. *Cold Spring Harb Symp Quant Biol*. 65:127-133.

Liu, C., Y. Kato, Z. Zhang, V.M. Do, B.A. Yankner, and X. He. 1999. beta-Trcp couples beta-catenin phosphorylation-degradation and regulates Xenopus axis formation. *Proc Natl Acad Sci U S A*. 96:6273-6278.

Liu, C., Y. Li, M. Semenov, C. Han, G.H. Baeg, Y. Tan, Z. Zhang, X. Lin, and X. He. 2002. Control of beta-catenin phosphorylation/degradation by a dual-kinase mechanism. *Cell*. 108:837-847.

Liu, Q., S. Guntuku, X.S. Cui, S. Matsuoka, D. Cortez, K. Tamai, G. Luo, S. Carattini-Rivera, F. DeMayo, A. Bradley, L.A. Donehower, and S.J. Elledge.

2000. Chk1 is an essential kinase that is regulated by Atr and required for the G(2)/M DNA damage checkpoint. *Genes Dev*. 14:1448-1459.

Lomonosov, M., S. Anand, M. Sangrithi, R. Davies, and A.R. Venkitaraman. 2003. Stabilization of stalled DNA replication forks by the BRCA2 breast cancer susceptibility protein. *Genes Dev*. 17:3017-3022.

Lopes, M., C. Cotta-Ramusino, A. Pellicioli, G. Liberi, P. Plevani, M. Muzi-Falconi, C.S. Newlon, and M. Foiani. 2001. The DNA replication checkpoint response stabilizes stalled replication forks. *Nature*. 412:557-561.

Lord, C.J., and A. Ashworth. 2012. The DNA damage response and cancer therapy. *Nature*. 481:287-294.

Lord, C.J., and A. Ashworth. 2016. BRCAness revisited. *Nat Rev Cancer*. 16:110-120.

Lowndes, N.F., and J.R. Murguia. 2000. Sensing and responding to DNA damage. *Curr Opin Genet Dev*. 10:17-25.

Martinez, A. 2008. Preclinical efficacy on GSK-3 inhibitors: towards a future generation of powerful drugs. *Med Res Rev*. 28:773-796.

McCubrey, J.A., L.S. Steelman, F.E. Bertrand, N.M. Davis, M. Sokolosky, S.L. Abrams, G. Montalto, A.B. D'Assoro, M. Libra, F. Nicoletti, R. Maestro, J. Basecke, D. Rakus, A. Gizak, Z.N. Demidenko, L. Cocco, A.M. Martelli, and M. Cervello. 2014. GSK-3 as potential target for therapeutic intervention in cancer. *Oncotarget*. 5:2881-2911.

Meijer, L., M. Flajolet, and P. Greengard. 2004. Pharmacological inhibitors of glycogen synthase kinase 3. *Trends Pharmacol Sci*. 25:471-480.

Melo, J., and D. Toczyski. 2002. A unified view of the DNA-damage checkpoint. *Curr Opin Cell Biol*. 14:237-245.

Mine-Hattab, J., and R. Rothstein. 2012. Increased chromosome mobility facilitates homology search during recombination. *Nat Cell Biol*. 14:510-517.

Moreno-Herrero, F., M. de Jager, N.H. Dekker, R. Kanaar, C. Wyman, and C. Dekker. 2005. Mesoscale conformational changes in the DNA-repair complex Rad50/Mre11/Nbs1 upon binding DNA. *Nature*. 437:440-443.

Morin, P.J., A.B. Sparks, V. Korinek, N. Barker, H. Clevers, B. Vogelstein, and K.W. Kinzler. 1997. Activation of beta-catenin-Tcf signaling in colon cancer by mutations in beta-catenin or APC. *Science*. 275:1787-1790.

Moynahan, M.E., A.J. Pierce, and M. Jasin. 2001. BRCA2 is required for homology-directed repair of chromosomal breaks. *Mol Cell*. 7:263-272.

Murga, M., S. Campaner, A.J. Lopez-Contreras, L.I. Toledo, R. Soria, M.F. Montana, L. D'Artista, T. Schleker, C. Guerra, E. Garcia, M. Barbacid, M. Hidalgo, B. Amati, and O. Fernandez-Capetillo. 2011. Exploiting oncogene-induced

replicative stress for the selective killing of Myc-driven tumors. *Nat Struct Mol Biol*. 18:1331-1335.

Nagaraju, G., and R. Scully. 2007. Minding the gap: the underground functions of BRCA1 and BRCA2 at stalled replication forks. *DNA Repair (Amst)*. 6:1018-1031.

Negrini, S., V.G. Gorgoulis, and T.D. Halazonetis. 2010. Genomic instability--an evolving hallmark of cancer. *Nat Rev Mol Cell Biol*. 11:220-228.

Nimonkar, A.V., J. Genschel, E. Kinoshita, P. Polaczek, J.L. Campbell, C. Wyman, P. Modrich, and S.C. Kowalczykowski. 2011. BLM-DNA2-RPA-MRN and EXO1-BLM-RPA-MRN constitute two DNA end resection machineries for human DNA break repair. *Genes Dev*. 25:350-362.

Nimonkar, A.V., A.Z. Ozsoy, J. Genschel, P. Modrich, and S.C. Kowalczykowski. 2008. Human exonuclease 1 and BLM helicase interact to resect DNA and initiate DNA repair. *Proc Natl Acad Sci U S A*. 105:16906-16911.

Novak, A., and S. Dedhar. 1999. Signaling through beta-catenin and Lef/Tcf. *Cell Mol Life Sci*. 56:523-537.

Okada, N., Y. Kitano, and K. Ichihara. 1982. Effects of cholera toxin on proliferation of cultured human keratinocytes in relation to intracellular cyclic AMP levels. *J Invest Dermatol*. 79:42-47.

Pacek, M., and J.C. Walter. 2004. A requirement for MCM7 and Cdc45 in chromosome unwinding during eukaryotic DNA replication. *EMBO J*. 23:3667-3676.

Patel, S., and J. Woodgett. 2008. Glycogen synthase kinase-3 and cancer: good cop, bad cop? *Cancer Cell*. 14:351-353.

Pei, J.J., T. Tanaka, Y.C. Tung, E. Braak, K. Iqbal, and I. Grundke-Iqbal. 1997. Distribution, levels, and activity of glycogen synthase kinase-3 in the Alzheimer disease brain. *J Neuropathol Exp Neurol*. 56:70-78.

Petermann, E., and T. Helleday. 2010. Pathways of mammalian replication fork restart. *Nat Rev Mol Cell Biol*. 11:683-687.

Pierce, S.B., and D. Kimelman. 1995. Regulation of Spemann organizer formation by the intracellular kinase Xgsk-3. *Development*. 121:755-765.

Plyte, S.E., K. Hughes, E. Nikolakaki, B.J. Pulverer, and J.R. Woodgett. 1992. Glycogen synthase kinase-3: functions in oncogenesis and development. *Biochim Biophys Acta*. 1114:147-162.

Polakis, P. 1999. The oncogenic activation of beta-catenin. *Curr Opin Genet Dev*. 9:15-21.

Prakash, R., Y. Zhang, W. Feng, and M. Jasin. 2015. Homologous recombination and human health: the roles of BRCA1, BRCA2, and associated proteins. *Cold Spring Harb Perspect Biol*. 7:a016600.

Ragland, R.L., S. Patel, R.S. Rivard, K. Smith, A.A. Peters, A.K. Bielinsky, and E.J. Brown. 2013. RNF4 and PLK1 are required for replication fork collapse in ATR-deficient cells. *Genes Dev*. 27:2259-2273.

Ray Chaudhuri, A., E. Callen, X. Ding, E. Gogola, A.A. Duarte, J.E. Lee, N. Wong, V. Lafarga, J.A. Calvo, N.J. Panzarino, S. John, A. Day, A.V. Crespo, B. Shen, L.M. Starnes, J.R. de Ruiter, J.A. Daniel, P.A. Konstantinopoulos, D. Cortez, S.B. Cantor, O. Fernandez-Capetillo, K. Ge, J. Jonkers, S. Rottenberg, S.K. Sharan, and A. Nussenzweig. 2016. Replication fork stability confers chemoresistance in BRCA-deficient cells. *Nature*. 535:382-387.

Rayasam, G.V., V.K. Tulasi, R. Sodhi, J.A. Davis, and A. Ray. 2009. Glycogen synthase kinase 3: more than a namesake. *Br J Pharmacol*. 156:885-898.

Reaban, M.E., and J.A. Griffin. 1990. Induction of RNA-stabilized DNA conformers by transcription of an immunoglobulin switch region. *Nature*. 348:342-344.

Reaban, M.E., J. Lebowitz, and J.A. Griffin. 1994. Transcription induces the formation of a stable RNA.DNA hybrid in the immunoglobulin alpha switch region. *J Biol Chem*. 269:21850-21857.

Rubinfeld, B., I. Albert, E. Porfiri, S. Munemitsu, and P. Polakis. 1997. Loss of beta-catenin regulation by the APC tumor suppressor protein correlates with loss of structure due to common somatic mutations of the gene. *Cancer Res*. 57:4624-4630.

Sakai, W., E.M. Swisher, B.Y. Karlan, M.K. Agarwal, J. Higgins, C. Friedman, E. Villegas, C. Jacquemont, D.J. Farrugia, F.J. Couch, N. Urban, and T. Taniguchi. 2008. Secondary mutations as a mechanism of cisplatin resistance in BRCA2-mutated cancers. *Nature*. 451:1116-1120.

Sartori, A.A., C. Lukas, J. Coates, M. Mistrik, S. Fu, J. Bartek, R. Baer, J. Lukas, and S.P. Jackson. 2007. Human CtIP promotes DNA end resection. *Nature*. 450:509-514.

Schlacher, K., N. Christ, N. Siaud, A. Egashira, H. Wu, and M. Jasin. 2011. Double-strand break repair-independent role for BRCA2 in blocking stalled replication fork degradation by MRE11. *Cell*. 145:529-542.

Schlacher, K., H. Wu, and M. Jasin. 2012. A distinct replication fork protection pathway connects Fanconi anemia tumor suppressors to RAD51-BRCA1/2. *Cancer Cell*. 22:106-116.

Segurado, M., M. Gomez, and F. Antequera. 2002. Increased recombination intermediates and homologous integration hot spots at DNA replication origins. *Mol Cell*. 10:907-916.

Shiloh, Y. 2003. ATM and related protein kinases: safeguarding genome integrity. *Nat Rev Cancer*. 3:155-168.

Simsek, D., and M. Jasin. 2010. Alternative end-joining is suppressed by the canonical NHEJ component Xrcc4-ligase IV during chromosomal translocation formation. *Nat Struct Mol Biol*. 17:410-416.

Stambolic, V., and J.R. Woodgett. 1994. Mitogen inactivation of glycogen synthase kinase-3 beta in intact cells via serine 9 phosphorylation. *Biochem J*. 303 (Pt 3):701-704.

Stampfer, M.R. 1982. Cholera toxin stimulation of human mammary epithelial cells in culture. *In Vitro*. 18:531-537.

Stracker, T.H., J.W. Theunissen, M. Morales, and J.H. Petrini. 2004. The Mre11 complex and the metabolism of chromosome breaks: the importance of communicating and holding things together. *DNA Repair (Amst)*. 3:845-854.

Sung, P. 1994. Catalysis of ATP-dependent homologous DNA pairing and strand exchange by yeast RAD51 protein. *Science*. 265:1241-1243.

Sung, P., and D.L. Robberson. 1995. DNA strand exchange mediated by a RAD51-ssDNA nucleoprotein filament with polarity opposite to that of RecA. *Cell*. 82:453-461.

Sutherland, C., I.A. Leighton, and P. Cohen. 1993. Inactivation of glycogen synthase kinase-3 beta by phosphorylation: new kinase connections in insulin and growth-factor signalling. *Biochem J*. 296 (Pt 1):15-19.

Suzuki, A., J.L. de la Pompa, R. Hakem, A. Elia, R. Yoshida, R. Mo, H. Nishina, T. Chuang, A. Wakeham, A. Itie, W. Koo, P. Billia, A. Ho, M. Fukumoto, C.C. Hui, and T.W. Mak. 1997. Brca2 is required for embryonic cellular proliferation in the mouse. *Genes Dev*. 11:1242-1252.

Sy, S.M., M.S. Huen, and J. Chen. 2009a. PALB2 is an integral component of the BRCA complex required for homologous recombination repair. *Proc Natl Acad Sci U S A*. 106:7155-7160.

Sy, S.M., M.S. Huen, Y. Zhu, and J. Chen. 2009b. PALB2 regulates recombinational repair through chromatin association and oligomerization. *J Biol Chem*. 284:18302-18310.

Tacconi, E.M.C. 2015. Novel approaches for targeting BRCA2-deficient tumour cells. *In* Department of Oncology. Vol. DPhil. University of Oxford. 296.

Takahashi-Yanaga, F. 2013. Activator or inhibitor? GSK-3 as a new drug target. *Biochem Pharmacol*. 86:191-199.

Tang, W., M. Dodge, D. Gundapaneni, C. Michnoff, M. Roth, and L. Lum. 2008. A genome-wide RNAi screen for Wnt/beta-catenin pathway components identifies unexpected roles for TCF transcription factors in cancer. *Proc Natl Acad Sci U S A*. 105:9697-9702.

Tercero, J.A., and J.F. Diffley. 2001. Regulation of DNA replication fork progression through damaged DNA by the Mec1/Rad53 checkpoint. *Nature*. 412:553-557.

Thompson, S.L., and D.A. Compton. 2011. Chromosome missegregation in human cells arises through specific types of kinetochore-microtubule attachment errors. *Proc Natl Acad Sci U S A*. 108:17974-17978.

Tkac, J., G. Xu, H. Adhikary, J.T. Young, D. Gallo, C. Escribano-Diaz, J. Krietsch, A. Orthwein, M. Munro, W. Sol, A. Al-Hakim, Z.Y. Lin, J. Jonkers, P. Borst, G.W. Brown, A.C. Gingras, S. Rottenberg, J.Y. Masson, and D. Durocher. 2016. HELB Is a Feedback Inhibitor of DNA End Resection. *Mol Cell*. 61:405-418.

Tutt, A., M. Robson, J.E. Garber, S.M. Domchek, M.W. Audeh, J.N. Weitzel, M. Friedlander, B. Arun, N. Loman, R.K. Schmutzler, A. Wardley, G. Mitchell, H. Earl, M. Wickens, and J. Carmichael. 2010. Oral poly(ADP-ribose) polymerase inhibitor olaparib in patients with BRCA1 or BRCA2 mutations and advanced breast cancer: a proof-of-concept trial. *Lancet*. 376:235-244.

Valerie, K., and L.F. Povirk. 2003. Regulation and mechanisms of mammalian double-strand break repair. *Oncogene*. 22:5792-5812.

Valko, M., C.J. Rhodes, J. Moncol, M. Izakovic, and M. Mazur. 2006. Free radicals, metals and antioxidants in oxidative stress-induced cancer. *Chem Biol Interact*. 160:1-40.

Welcsh, P.L., and M.C. King. 2001. BRCA1 and BRCA2 and the genetics of breast and ovarian cancer. *Hum Mol Genet*. 10:705-713.

WHO. 2017. Cancer Fact Sheet. World Health Organisation.

Wiederschain, D., S. Wee, L. Chen, A. Loo, G. Yang, A. Huang, Y. Chen, G. Caponigro, Y.M. Yao, C. Lengauer, W.R. Sellers, and J.D. Benson. 2009. Single-vector inducible lentiviral RNAi system for oncology target validation. *Cell Cycle*. 8:498-504.

Winston, J.T., P. Strack, P. Beer-Romero, C.Y. Chu, S.J. Elledge, and J.W. Harper. 1999. The SCFbeta-TRCP-ubiquitin ligase complex associates specifically with phosphorylated destruction motifs in IkappaBalpha and beta-catenin and stimulates IkappaBalpha ubiquitination in vitro. *Genes Dev*. 13:270-283.

Woodgett, J.R. 1990. Molecular cloning and expression of glycogen synthase kinase-3/factor A. *EMBO J*. 9:2431-2438.

Xu, G., J.R. Chapman, I. Brandsma, J. Yuan, M. Mistrik, P. Bouwman, J. Bartkova, E. Gogola, D. Warmerdam, M. Barazas, J.E. Jaspers, K. Watanabe, M. Pieterse, A. Kersbergen, W. Sol, P.H. Celie, P.C. Schouten, B. van den Broek, A. Salman, M. Nieuwland, I. de Rink, J. de Ronde, K. Jalink, S.J. Boulton, J. Chen, D.C. van Gent, J. Bartek, J. Jonkers, P. Borst, and S. Rottenberg. 2015. REV7 counteracts DNA double-strand break resection and affects PARP inhibition. *Nature*. 521:541-544.

Yazinski, S.A., V. Comaills, R. Buisson, M.M. Genois, H.D. Nguyen, C.K. Ho, T. Todorova Kwan, R. Morris, S. Lauffer, A. Nussenzweig, S. Ramaswamy, C.H. Benes, D.A. Haber, S. Maheswaran, M.J. Birrer, and L. Zou. 2017. ATR inhibition disrupts rewired homologous recombination and fork protection pathways in PARP inhibitor-resistant BRCA-deficient cancer cells. *Genes Dev*. 31:318-332.

Yoshino, Y., and C. Ishioka. 2015. Inhibition of glycogen synthase kinase-3 beta induces apoptosis and mitotic catastrophe by disrupting centrosome regulation in cancer cells. *Sci Rep*. 5:13249.

Zeman, M.K., and K.A. Cimprich. 2014. Causes and consequences of replication stress. *Nat Cell Biol*. 16:2-9.

Zeng, X., H. Huang, K. Tamai, X. Zhang, Y. Harada, C. Yokota, K. Almeida, J. Wang, B. Doble, J. Woodgett, A. Wynshaw-Boris, J.C. Hsieh, and X. He. 2008. Initiation of Wnt signaling: control of Wnt coreceptor Lrp6 phosphorylation/activation via frizzled, dishevelled and axin functions. *Development*. 135:367-375.

Zhang, F., J. Ma, J. Wu, L. Ye, H. Cai, B. Xia, and X. Yu. 2009. PALB2 links BRCA1 and BRCA2 in the DNA-damage response. *Curr Biol*. 19:524-529.

Zhang, Y., and M. Jasin. 2011. An essential role for CtIP in chromosomal translocation formation through an alternative end-joining pathway. *Nat Struct Mol Biol*. 18:80-84.

Zhao, H., and H. Piwnica-Worms. 2001. ATR-mediated checkpoint pathways regulate phosphorylation and activation of human Chk1. *Mol Cell Biol*. 21:4129-4139.

Zimmer, J., E.M. Tacconi, C. Folio, S. Badie, M. Porru, K. Klare, M. Tumiati, E. Markkanen, S. Halder, A. Ryan, S.P. Jackson, K. Ramadan, S.G. Kuznetsov, A. Biroccio, J.E. Sale, and M. Tarsounas. 2016. Targeting BRCA1 and BRCA2 Deficiencies with G-Quadruplex-Interacting Compounds. *Mol Cell*. 61:449-460.

Zonderland, G. 2016. GSK3 inhibition selectively eliminates BRCA-deficient cells. *In* Molecular Biology. Vol. BSc. Hogeschool Leiden. 37.

Zou, L., and S.J. Elledge. 2003a. Sensing DNA damage through ATRIP recognition of RPA-ssDNA complexes. *Science*. 300:1542-1548.

Zou, L., D. Liu, and S.J. Elledge. 2003b. Replication protein A-mediated recruitment and activation of Rad17 complexes. *Proc Natl Acad Sci U S A*. 100:13827-13832.

6 Appendix

Original copyright notices